Low-frequency, low-magnitude vibrations (LFLM) enhances chondrogenic differentiation potential of human adipose derived mesenchymal stromal stem cells (hASCs)

Krzysztof Marycz, Daniel Lewandowski, Krzysztof A Tomaszewski, Brandon Michael Henry, Edward B Golec, Monika Marędziak

The aim of this study was to evaluate if low-frequency, low-magnitude vibrations (LFLM) could enhance chondrogenic differentiation potential of human adipose derived mesenchymal stem cells (hASCs) with simultaneous inhibition of their adipogenic properties for biomedical purposes. We developed a prototype device that induces low-magnitude (0.3 g) low-frequency vibrations with the following frequencies: 25, 35 and 45 Hz. Afterwards, we used human adipose derived mesenchymal stem cell (hASCS), to investigate their cellular response to the mechanical signals. We have also evaluated hASCs morphological and proliferative activity changes in response to each frequency. Induction of chondrogenesis in hASCs, under the influence of a 35 Hz signal leads to most effective and stable cartilaginous tissue formation through highest secretion of Bone Morphogenetic Protein 2 (BMP-2), and Collagen type II, with low concentration of Collagen type I. These results correlated well with appropriate gene expression level. Simultaneously, we observed significant up-regulation of $\alpha 3$, $\alpha 4$, $\beta 1$ and $\beta 3$ integrins in chondroblast progenitor cells treated with 35Hz vibrations, as well as Sox-9. Interestingly, we noticed that application of 35 Hz frequencies significantly inhibited adipogenesis of hASCs. The obtained results suggest that application of LFLM vibrations together with stem cell therapy might be a promising tool in cartilage regeneration.

1 **Low-frequency, low-magnitude vibrations (LFLM) enhances chondrogenic differentiation**

2 **potential of human adipose derived mesenchymal stromal stem cells (hASCs).**

4 Krzysztof Marycz [1, 2], Daniel Lewandowski [3], Krzysztof A Tomaszewski [4, 5], Brandon Michael

5 Henry [4], Edward B. Golec [5, 6], Monika Marędziak [7]

7 1. Faculty of Biology, University of Environmental and Life Sciences, Kozuchowska 5b St, 50-

8   631 Wroclaw, Poland

9 2. Wroclaw Research Centre EIT +, Stablowicka 147 St, 54-066 Wroclaw, Poland

10 3. Institute of Materials Science and Applied Mechanics, University of Technology,

11   Smoluchowskiego 25 St, 50-370 Wroclaw, Poland

12 4. Department of Anatomy, Jagiellonian University Medical College, Kopernika 12 St, 31-034

13   Krakow, Poland

14 5. Department of Orthopaedics and Trauma Surgery, 5th Military Clinical Hospital and

15   Polyclinic, Krakow, Poland

16 6. Orthopaedic Rehabilitation Department, Chair of Clinical Rehabilitation, Bronislaw Czech

17   Academy of Physical Education, Krakow, Poland

18 7. Faculty of Veterinary Medicine, Department of Animal Physiology and Biostructure

19   University of Environmental and Life Sciences, Norwida 31 St, 50-375 Wroclaw, Poland

21 **Corresponding author**: Krzysztof Marycz, Electron Microscopy Laboratory, Kożuchowska 5b,

22 51-631 Wroclaw, Poland , krzysztofmarycz@interia.pl

24 **Abstract**

25 The aim of this study was to evaluate if low-frequency, low-magnitude vibrations (LFLM) could

26 enhance chondrogenic differentiation potential of human adipose derived mesenchymal stem

27 cells (hASCs) with simultaneous inhibition of their adipogenic properties for biomedical

28 purposes. We developed a prototype device that induces low-magnitude (0.3 g) low-frequency

29 vibrations with the following frequencies: 25, 35 and 45 Hz. Afterwards, we used human adipose

30 derived mesenchymal stem cell (hASCS), to investigate their cellular response to the mechanical

31 signals. We have also evaluated hASCs morphological and proliferative activity changes in

32 response to each frequency. Induction of chondrogenesis in hASCs, under the influence of a 35

33 Hz signal leads to most effective and stable cartilaginous tissue formation through highest

34 secretion of Bone Morphogenetic Protein 2 (BMP-2), and Collagen type II, with low

35 concentration of Collagen type I. These results correlated well with appropriate gene expression

36 level. Simultaneously, we observed significant up-regulation of α3, α4, β1 and β3 integrins in

37 chondroblast progenitor cells treated with 35Hz vibrations, as well as Sox-9. Interestingly, we

38 noticed that application of 35 Hz frequencies significantly inhibited adipogenesis of hASCs. The

39 obtained results suggest that application of LFLM vibrations together with stem cell therapy

40 might be a promising tool in cartilage regeneration.

42 **Introduction**

43 Articular cartilage injuries are a growing problem in both human and veterinary medicine. Injury

44 to cartilage manifests through the typical signs of inflammation, and can be caused by either

45 trauma or diseases such as osteonecrosis, cartilage necrosis, or arthritis. Because cartilage is an

46 avascular tissue with chondrocytes that are characterized by a low mitotic potential, the

47 regenerative potential cartilage is substantially limited [1]. As such, the spontaneous regeneration

48 of injured cartilage is extremely difficult. Until recently, the vast majority of the available

49 treatment methods have focused on eliminating symptoms and improving patient quality-of-life

50 through the use steroidal or non-steroidal anti-inflammatory drug treatment (NSAIDs) [2].

51 However, when used long-term, these medications may lead to chondronecrosis [3].

52 A potential solution to this problem emerges in the form of cell based therapies. Adult

53 mesenchymal stem cells (MSCs) may be a possible source of cells for this type of therapy due to

54 their immunomodulatory action, ability to self-renew, and ability to differentiate into several cell

55 lineages, i.e. chondrocytes, osteoblasts or adipocytes [4, 5]. Currently, bone marrow (BMMSCs)

56 and adipose derived mesenchymal stem cells (ASCs) are the cells most frequently applied in

57 cell-based therapies at the preclinical stage. Of the two cell types mentioned above, ASCs seem a

58 better alternative to BMMSCs, due to their easy accessibility, and thus lower donor-related risks

59 [6]. Moreover, activated ASCs secrete from their surface small, spherical membrane fragments

60 called microvesicles (MVs) [7]. These MVs contain important regenerative molecules, that

61 improve the function of damaged tissues - eg. growth factors, bioactive lipids, proteins.

62 Microvesicles secreted by MSCs, stimulated to differentiate into osteocytes, release into the

63 culture medium compounds rich in Collagen type I and II or Bone Morphogenetic Protein 2 [8,

64   9]. Several studies have confirmed the beneficial clinical effect of ASCs in the treatment of

65   musculoskeletal disorders, particularly in the field of veterinary orthopedics [10, 11, 12]. In our

66   previous study, we demonstrated the positive effects of ASCs application in equine and canine

67   osteoarthritis treatment [13].

68   However, one major limitation to the clinical application of ASCs is the age-related decrease in

69   the proliferative and chondrogenic differentiation potential of ASCs obtained from older

70   populations [14]. As degenerative joint diseases increase in prevalence with age, it is important

71   to develop methods to overcome this limitation. In order to improve both the proliferative and

72   the differentiation potential of ASCs, various physical stimuli such as static magnetic field [15],

73   electric signals [16] and cyclic strain [17] have been applied. However, this field still remains

74   relatively unexplored in terms of the biological effects of low-magnitude low-frequency

75   vibration (LMLF) - a non-invasive biophysical intervention that leads to cyclic loading of the

76   targeted tissue. LMLF vibrations include values of magnitude under 1.0 g, where g = 9,81 m/s²,

77   and a frequency between 20 – 100 Hz [18]. Several studies have investigated the role of various

78   magnitudes and frequencies of vibrations, such as high-magnitude low-frequency (HMLF)

79   vibrations [19], high-magnitude high frequency vibrations (HMHF) [20] and low-magnitude

80   high-frequency (LMHF) vibrations [21], in the context of their influence on cellular response

81   [22-26] . Moreover, it has been reported that LMHF enhance the osteogenic differentiation

82   potential of MSCs [20]. Enhancement of osteogenic and/or chondrogenic differentiation

83   potential of MSCs may strongly depend on up-regulation of particular integrins, that are

84   activated by various biomechanical signals [27] . Integrins are heterodimeric glycoproteins that

85   are composed of an α- and a β-subunit, each of which has an extracellular and a cytoplasmic

86   domain [28]. Several studies have provided evidence that chondrocytes express integrins [29-

87   34]. In particular, the α1β1 and α5β1 integrins have been shown to be the most prominent in

88   adult chondrocytes isolated from normal articular cartilage. However, the other integrins are still

89   poorly investigated, especially in the context of their expression in differentiated precursor cells

90   additionally stimulated by various types of external mechanical or others signals.

91   In an animal model, LMHF signals had a positive influence on both bone formation and density,

92   enhancing bone strength and recovery after bone fracture [35, 36, 37]. Moreover, preliminary

93   studies in children with disabling conditions and post-menopausal women indicate that such

94   signals can be efficacious in reversing and/or preventing bone loss [37]. However, to the best

95   knowledge of the authors, the current literature lacks data concerning the effects of LMLF

96   vibrations on the chondrogenic differentiation potential of human ASCs.

97   The aim of this study was to investigate how harmonic vibration, sinusoidal with constant low-

98   magnitude (0.3g, where g = 9,81 m/s^2) and low-frequency (25, 35, 45 Hz) mechanical signals,

99   generated by an actuating device, effects ASC morphology, growth, and adipogenic and

100   chondrogenic differentiation potential.

102   **Materials and Methods**

103   ***Description of the cell vibration generator prototype***

104   The process of inducing vibrations was applied using custom-made vibration platforms, specially

105   constructed device that allowed to induce mechanical motion of a 24-well culture plate.

106   Movement of the plate was characterized by the harmonic sine of a given amplitude and

107   frequency. The direction of plate translations was perpendicular to the main surface on which the

108   cells were cultured.

109   A scheme of the stand is shown in Fig. 1C and photographs in Figure 1A, 1B. The vibration

110   generator, an electromagnetic actuator, is positioned on a stationary base. The principle of its

111   operation is based on coil movement, which is generated by an alternating current flow. The

112   design of the actuator is similar to that of a typical loudspeaker, with the main difference being

113   that the moving parts are not a flexible membrane but a stiff plate.

114   The stiff plate of the actuator moves in a linear manner in relation to the stationary part. Fig. 1C

115   depicts the displacement value as 'x'. Between the actuator and the culture plate, a spacer has

116   been mounted. The spacer is a rigid element made of polyethylene, placed to create distance

117   from the cell culture actuator. This was done to eliminate the possible influence of the alternating

118   magnetic field generated by the EM-actuator on the cell culture. The height of the spacer was

119   about 10 cm. The strength of the magnetic field at this distance does not differ from the

120   background.

121   The culture plate was attached to the top surface of the spacer in such a way to allow quick

122   mounting. Such a method was dictated by the fact that the vibration stimulation was scheduled

123   only for short periods of time each day. Movement of the culture plate was defined as a course of

124   the sine function with a given value of frequency and amplitude of acceleration. A laser

125 displacement sensor (KEYENCE LK-G157) was used to measure the translation of the culture

126 plate. The acceleration signal was calculated according to the following formula:

$$x = A sin(\omega t) \quad \rightarrow \quad \ddot{x} = -A\omega^2 sin(\omega t)$$

128 where x – displacement, $\ddot{x}$ – acceleration, A – amplitude of displacement, ω – frequency of vibrations ($\omega = 2\pi f$), f

129 – frequency, t – time, $A\omega^2$ – amplitude of acceleration.

Vibration loading protocol of hASCs culture

131 The hASCs were seeded at a concentration of 3×10^4 on 24 - well plates and 5 x 10^4 to a 15 ml

132 tube. Tubes with 3D model were vibrated on tube rack. For each vibration model (25, 35 and

133 45Hz) separate dishes were used. Plates/racks were placed securely onto the vibration device

134 and oscillated vertically at 25, 35 and 45 Hz. The stimulus was sinusoidal and delivered with a

135 peak acceleration of 0,3 g for 15 minutes once a day, for 14 consecutive days. Cells in the non-

136 vibration group were placed on the same but stationary plate. After 15 min of vibration, the

137 hASCs (both vibrated and non-vibrated groups) received fresh culture medium.

Isolation of human adipose derived mesenchymal stem cells (hASCs)

139 This study was approved by the local bioethics committee of Wroclaw Medical University,

140 Poland (number KB-177/2014). Written informed consent was obtained from each patient prior

141 to tissue collection during total hip arthroplasty. This study adhered to the Helsinki Declaration

142 (1964) and its later amendments.

143 Subcutaneous adipose tissue was collected from 4 patients. From each patient we obtained 4

144 donor samples, representing of a total n=16. The average age of the patients was 69±1 years.

145 Briefly, after collection, the tissue samples were placed in sterile Hank's Balanced Salt Solution

146 (HBSS). The isolation procedure of adipose-derived mesenchymal stem cells was conducted

147   under aseptic conditions and in accordance with previously described protocol [38, 39]. Samples

148   were washed with HBSS supplemented with a 1% antibiotic-antimicotic solution

149   (penicillin/streptomycin/amphotericin b at a concentration of 0.017mol/l, 0.01mol/l and

150   0.0002mol/l respectively; Sigma Aldrich, cat no A5955) and then cut into small pieces using

151   surgical scissors. Next, the samples were placed in a sterile centrifuge tube and digested with

152   type I collagenase (1 mg/ml, Sigma Aldrich, cat no C5894). After 30 minutes incubation at 37°C,

153   the tissue homogenate was centrifuged at 1200g for 10 minutes. The supernatant was removed

154   and the cell pellet was resuspended in growth media. The cell suspension was then transferred to

155   the cell culture flask.

156   ***Immunophenotyping, Fluorescence-activated cell sorting (FACs) analysis, and multipotency***

157   ***test***

158   Cells were plated on 24-well culture plates suspended in 500 μl of standard medium at a

159   concentration of 8 x 10^3 cells per well. The presence of specific antigens for ASCs, i.e. integrin

160   beta-1 (CD29), HCAM (CD44), 5'-nucleotidase (CD73) and endoglin (CD105) and leukocyte

161   common antigen (CD45) was examined after one week of culture by means of primary

162   antibodies (all from Sigma Aldrich). Negative staining of CD45 was used to exclude

163   hematopoietic origin. After fixation, cells were permeabilized with 0,2% Tween 20 for 15

164   minutes and washed three times with HBSS. The solution of primary antibody and 4% FBS in

165   PBS was applied to every well and incubated overnight at 4°C. Next, the cells were washed three

166   times and secondary goat anti-rabbit conjugated with Atto 488 antibody was added to

167   appropriate wells at concentration 1:150. After incubation at room temperature for 1.5 hours, the

168   cells were washed again and photographed under a fluorescence microscope.

169 For the multipotency test, cells were cultured on chondrogenic and adipogenic media

170 (STEMPRO® Chondrogenesis/Osteogenesis Differentiation Kit and STEMPRO® Adipogenesis

171 Differentiation Kit, Life Technologies) for 14 days. The culture media was changed every

172 second day.

173 After 3 passages, the ASCs were examined for surface protein molecule expression by flow

174 cytometry. Cells were trypinized using a Trypsin-EDTA solution (TrypLE™, Life

175 Technologies), centrifuged at 400 xg for 3 minutes, and then washed with PBS containing 2%

176 FBS (fetal bovine serum) (Sigma Aldrich). A total of 5 x 10^5 cells were labeled for 20 min (on

177 ice and dark) with antibodies pre-conjugated with allophycocyanin (APC), peridinin

178 chlorphyllprotein (PerCP), fluorescein isothiocyanate (FITC) or phycoerythrin (PE). The

179 following CD surface markers were tested: CD34, CD45, CD105, CD90, CD73, CD44, CD29

180 and IgG1 as an isotype control antibody (BD Pharmingen). The samples were analyzed by a

181 Becton Dickinson FACSCalibur flow cytometer. At least ten thousand events were acquired for

182 each CD surface marker. The data was then analyzed using FlowJo X software (Treestar).

183 ***Cell culture***

184 Throughout the experiment, hASCs were cultured in aseptic and constant conditions in an

185 incubator at 37°C, 5% CO_2 and 95% humidity. The cell population was plated in T-75 culture

186 flasks for primary culture and was maintained in Dulbecco's Modified Eagle's Medium

187 (DMEM) with nutrient F-12 Ham (Sigma Aldrich) supplemented with 10% FBS and 1% of

188 antibiotic/antimicotic solution at a concentration of 0,017mol/l, 0,01mol/l and 0,0002mol/l

189 respectively (Sigma Aldrich, cat no A5955). The culture medium was changed every second day.

190 Human ASCs were passaged using Trypsin-EDTA solution (TrypLE™, Life Technologies) in

191   accordance with manufacturer's instruction after reaching about 80-90% confluence. Cells were

192   passaged three times before use in experiments.

193   Isolated adipose-derived mesenchymal stem cells were divided into 2 groups. The first one was

194   stimulated with chondrogenic medium and the second one with adipogenic medium. The

195   differentiation processes of hASCs were performed using the STEMPRO® Chondrogenesis

196   Differentiation Kit and STEMPRO® Adipogenesis Differentiation Kit (Life Technologies),

197   respectively. Cells were seeded at 3×10^4 on 24 - well plates and 5×10^4 to a 15 ml tube..The

198   stimulation of cells was performed in accordance with the manufacturers' instruction.

199   The chondrogenic culture was maintained in two systems: 2D in 24-well plates for fluorescent,

200   histochemical stainnings, rtPCR analysis and SEM, and 3D for ELISA tests and Focused Ion

201   Beam Scanning Electron Microscope (FIB-SEM, Auriga Compact Crossbeam, Zeiss, Germany).

202   For the 3D system, 2.5×10^5 hASCs were seeded into 15 ml polypropylene tubes and pelleted.

203   The hASCs were cultured for 14 days as 3D pellets in induction medium STEMPRO®

204   Chondrogenesis Differentiation Kit (Life Technologies). The experiment was repeated three

205   times. Both 2D and 3D cultures were incubated two days before starting vibration stimulation.

206   ***Cell proliferation assay***

207   The cell proliferation factor (PF) was evaluated using the Alamar Blue test (TOX-8, Sigma

208   Aldrich) according to the manufacturer's instructions. The culture media was replaced with a

209   medium containing 10% of resazurin-based dye and incubated for two hours. Afterwards, the

210   supernatants were collected and subjected to absorbance measurement by means of

211   spectrophotometer (SPECTRO StarNano, BMG Labtech) at 600 nm of wavelength, with a

212   distraction of 690 nm of background absorbance. The procedure was performed during the

213   differentiation period at days 2, 5, 10, and 14.

214   A standard curve obtained during the experiment, allowed to estimate the amount of cells. The

215   population doubling time (PDT) was assessed using an on-line calculator (http://www.doubling-

216   time.com/compute.php).

217   ***Examination of hASCs morphology***

218   Cell morphology, cellular composition, and culture growth pattern were analyzed using an

219   inverted, fluorescence microscope (AxioObserverA1, Zeiss) and a scanning electron microscope

220   (SEM; EVO LS15, Zeiss).

221   In order to begin observations, after the culture period, cells were fixed with 4%

222   paraformaldehyde. After 15-minutes permeabilization with 0.2% Tween, cells were stained using

223   atto-565-labeled phalloidin for 40 minutes to visualize actin filaments. After triple washing,

224   diamidino-2-phenylindole (DAPI) staining was applied for 5 min to analyze the distribution of

225   cell nuclei. All fluorescence staining was performed at room temperature in the dark.

226   Additionally, Oil Red O staining for adipogenic cultures and Safranin-O staining for

227   chondrogenic cultures were performed to observe fat droplets and chondrocytes, respectively.

228   After fixation, adipogenic samples were treated with 0.1% Oil Red O solution for 5 min, Plates

229   were rinsed 3x with water and images of cells on plate were taken. For quantification the

230   percentage of Oil Red O absorption, the dye was extracted by isopropanol and absorbance was

231   determined at 490 nm. Chondrogenic samples were treated with 1% acetic acid for 10 min and

232   stained with Safranin-O for 5 minutes. Images were acquired using a Cannon PowerShot digital

233   camera. In order to evaluate the chondrogenic differentiation efficiency, the concentration of

234   proteoglycans was determined, basing on the binding Safranin O to glycosaminoglycans and

235   spectrophotometric measurements at a 470 nm wavelength and assessment percentage of

236   Safranin O absorption. As 100% control, we adopted reagent not added to culture. To analyze

237   detailed morphological features of the cells, especially fat droplets, and chondrogenic nodules,

238   SEM was performed. After fixation, the cells were washed in distilled water and dehydrated in

239   ethanol (concentrations from 50 to 100%, every 5 min). Thoroughly dried cells were coated with

240   gold (ScanCoat 6, Oxford), placed in a microscope chamber, and observed using the SE1

241   detector, at 10 kV of filament's tension. To observe morphological features and measure

242   diameters of nodules (n=6) Ion Beam Scanning Electron Microscope (FIB-SEM, Auriga

243   Compact Crossbeam, Zeiss, Germany) obsrvations were performed. Analysis was performed

244   using a focus ion beam detector at magnification of 200X. Diameter of adipocytes (n=6) was

245   measured using Scanning Electron Microscope (SEM; EVO LS15, Zeiss).

246   ***Enzyme-linked immunosorbent assays***

247   In order to evaluate the chondrogenic differentiation efficiency on the protein level, the

248   concentration of chondrogenesis-specific markers was investigated. The total concentration of

249   proteins from pellet cultures was determined with enzyme-linked immunosorbent assay

250   (ELISA). For the analysis, cells homogenate were collected on the last day of the experiment.

251   Chondrogenic media was subjected to a BMP-2 ELISA assay (Bone Morphogenic Protein 2

252   Quantikine ELISA Kit, R&D Systems), and a Col-1 and a Col-2 ELISA assay (Human Collagen

253   alpha-1(I) and (II) chain ELISA Kit, EIAab). All steps of each ELISA tests were performed in

254   accordance with the manufacturer's protocol. Each sample was prepared in duplicate.

255   Spectrofotometric determination was performed using a microplate reader (Spectrostar Nano,

256   BMG Labtech) at a wavelength equal to 450 nm and with the correction wavelength of 540 nm.

257   The concentration of proteins was presented as a ratio of protein weight and supernatant volume

258   (w/v).

259   **Quantitative Real-Time Reverse Transcription Polymerase Chain Reaction (qRT-PCR)** In

260   order to analyze gene expression, cells after stimulation were rinsed with HBSS and were

261   homogenized with 0.5 ml of TRI Reagent (Sigma Aldrich) directly in the culture well. The total

262   RNA was isolated using a phenol-chloroform method as previously described [40]. After

263   isolation, total RNA was diluted in DEPC-treated water. The concentration and purity of RNA

264   preparations was determined by absorbance measured at 260 nm with a nanospectrophotometer

265   (VPA biowave II). Preparation of DNA-free RNA was performed using DNase I RNase-free kit

266   (Thermo Scientific). For each reaction, 100 ng of total RNA was used. Transcription of gDNA-

267   free total RNA to a complementary DNA (cDNA) was reverse transcribed using Moloney

268   Murine Leukemia Virus Reverse Transcriptase (M-MLV RT) and oligo(dT)15 primers

269   (Novazym). RNA purification and cDNA transcription was performed according to

270   manufacturers' instructions. Quantitative Real-Time polymerase chain reaction (qRT-PCR) was

271   performed using 5 μl of cDNA in total volume of 20 μl by means of SensiFast SYBR &

272   Fluorescein Kit (Bioline). The reaction was performed at a 500 nM final concentration of

273   primers. The primer sequences used are presented in Table 1. qRT-PCR was performed as

274   described previously [41]. Expression levels of all analyzed genes were normalized for the

275   expression level of glyceraldehyde-3-phosphate dehydrogenase (GAPDH), a housekeeping gene.

276   ***Statistical Analysis***

277   All experiments were performed with at least 3 (n=3) independent experiments (biological

278   replicates, n≥4) measured as quadriplicate or more (technical replicates, n≥4).").

279   Statistical analysis was performed using GraphPad Prism 5 software. The statistical significance

280   of results was calculated using the one-way analysis of variance (ANOVA) with post-hoc

281   Dunnett's test by means. A P-value of less than 0.05 was considered statistically significant.

282

283   **Results**

284   *hASCs - FACs analysis, immunophenotyping and multipotency test*

285   Flow cytometry analysis revealed that hASCs showed positive labeling for CD29, CD44, CD73,

286   CD105, and CD90 (Fig. 2B). The investigated cells were negatively labeled for two

287   hematopoietic markers: CD34 and CD45 (Fig. 2B). Additionally, immunohistochemical staining

288   confirmed the presence of mesenchymal markers (CD29, CD44, CD73, CD105) and excluded

289   hematopoietic origin (CD45) (Fig. 2A).

290   Moreover, the multipotent character of hASC's was confirmed by abundant osteogenic and

291   adipogenic differentiation. In contrast to cells cultured under control conditions, the presence of

292   osteo nodules, was observed in hASCs cultivated under osteogenic conditions (Fig. 2C).

293   Moreover, mineral calcium deposits visualized by Alizarin Red staining were clearly detected

294   after 3 weeks of osteogenic differentiation. After 2 weeks of culture with an adipogenic inducing

295   media, hASCs developed Oil Red O positive lipid droplets (Fig. 2C), whereas control cultures

296   grown in standard media failed to produce similar results (Fig. 2C).

297   *Proliferation rate (PF) and population doubling time (PDT) of 3D chondroblasts originated*

298   *from chondro induced hASCs.*

299   The proliferative activity, as well as the PDT, were analyzed during the 14 days of hASCs

300   culturing in chondrogenic induction medium exposed to vibration frequencies of 25, 35 and

301   45Hz and in non-vibration control conditions. The obtained data showed that all investigated

302   vibration frequencies influenced the proliferative potential, as well as the PDT, of chondroblasts

303   originated from hASCs (Fig. 3A, B). The percentage of Alamar Blue reduction decreased

304   proportionally with cell count and activity.

305   Cells cultured under 25 Hz frequency reached the highest PF after 2 days of incubation and then

306   declined, but on the 10th day of culture reached higher PF and declined again till the 14th day.

307   Moreover, we noticed the longest PDT (277±25 hours) when cells were stimulated with a 25Hz

308   frequency. The cells exposed to 35Hz vibrations had a higher PF than control cultures at all

309   investigated time points (Fig. 3A). During the analysis, hASCs after chondrogenic differentiation

310   using 25Hz vibrations resulted in the lowest proliferation potential, as well as longest PDT, when

311   compared to the other investigated groups.

312   ***The morphology of chondroblasts originated from hASCs***

313   After 14 days, formation of chondroblast-specific nodules could be clearly observed (Fig. 4A-P,

314   Fig. 5A-D, Panel B) and showed a strong orange signal after Safranin O staining (Fig. 4I-L).

315   Characteristic chondrocyte-like cells were observed in all of the investigated cultures, however,

316   the cells cultured under the influence of 35Hz vibrations more efficiently induced

317   chondrodifferentiation (Fig. 4N). In these samples, nodules had the largest size (Fig. 6A) as well

318   as exhibited the highest absorption of Safranin O (Fig. 6B). Cells cultured under 25Hz vibrations

319   absorbed less Safranin O dye and formed nodules with a significantly smaller diameter than

320   samples cultured with 35 Hz vibrations (Fig. 6A, B). Chondroinduction of cells treated with

321   45Hz were comparable to the control group. Although chondro-nodules had similar diameters,

322   the absorption of Safranin O by cells cultured with 45 Hz frequencies was significantly higher

323   (Fig. 6A, B).

324 ***Quantitative Collagen 1 and 2 (Col-1, Col-2) and Bone Morphogenetic Protein 2 (BMP-2)***

325 ***assay and chondrogenic gene expression analysis (SOX-9, Col-X, Col-II, Runx, Col-I, ACAN)***

326 The performed analysis showed an increase in collagen type 2 concentration in comparison to the

327 amount of collagen type I in all groups where vibrations were applied (Fig. 5A, B, Panel A).

328 These results were additionally confirmed by positive chondrogenic differentiation of hASCs.

329 The highest difference on mRNA level between collagen type II and type I was observed in the

330 cultures stimulated with 25 and 35 Hz vibrations, and in the control culture. The lowest

331 concentration of collagen type II with respect to collagen type I was observed when 45 Hz

332 frequency vibrations were applied (Fig. 5A, B, Panel A). Cells treated with 35Hz frequency

333 vibrations tended to secrete significantly higher amounts of BMP-2 in comparison to the other

334 groups (Fig. 5C, Panel A). Exposure to the 25Hz stimulation model resulted in secretion of lower

335 a concentration of BMP-2 in comparison to the 35Hz, however significantly higher when

336 compared to the 45Hz frequencies, as well as to the control culture.

337 The quantitative evaluation of the concentration of collagen type I and type II was additionally

338 confirmed by gene expression analysis (Fig. 4C, E, Panel A). The highest activity of collagen

339 type II and its predominance over expression of collagen type I was observed in cells treated

340 with 35Hz vibrations. Similarly to the quantitative evaluation, exposure to 25Hz vibrations

341 resulted in lower expression of Collagen type II when compared to the 35Hz vibrations model.

342 The gene expression of SOX-9 and Col-X, the master transcription factors of chondrogenesis,

343 gradually increased in 35 Hz treated cells compared to control group (Fig. 4A, B, Panel A).

344 Aggrecan (ACAN) and RUNX2, another chondrogenic markers, significantly increased after 25

345 Hz treatment (Fig. 4D, F, Panel A).

346 ***Analysis of integrin expression in response to vibration stimulation***

347 In order to sense and translate the applied external mechanical signals, cells express

348 mechanoreceptors on their surface, such as integrins. In our study, we analyzed the expression

349 changes of four alpha (α3, α 4, α 5 and αV) and three beta (β1, β3 and β5) integrin subunits (Fig.

350 7). qPCR analysis demonstrated a slight increase of integrin α3, α4, β1 and β3 subunit expression

351 after 25 Hz stimulation in comparison to control (0 Hz). We also found that when cells were

352 stimulated with 35 Hz vibrations, hASCs significantly upregulated integrin α3, α4, β1 and β3

353 subunit. Interestingly, after 35 Hz stimulation, the highest increase in expression of the β3

354 intergrin was observed. With respect to integrin subunits α5, αV, and β5, expression levels were

355 similar between to stimulated groups, however down-regulated as compared to control.

356 ***Proliferation factor and population doubling time of human adipocytes originated from adipo***

357 ***induced hASCs.***

358 The proliferation factor and PDT were determined in the various groups after 14 days of

359 adipogenic induction. The stimulated cultures were characterized by an irregular proliferation

360 rate (Fig. 8A). Stimulation with a 25 Hz frequency resulted in an increase of PF when compared

361 with the other groups. The highest PF was on day 5, and from that point on a decreasing trend

362 was observed (Fig. 8A). The 25Hz frequency group also has the shortest PDT in comparison to

363 other experimental groups (Fig. 8B).

364 In the 35Hz and 45 Hz treatment groups, proliferation remained decreased at days 2, 5 and 10 of

365 culture in comparison to the control and 25 Hz group, although this difference was not as

366 pronounced as that on day 14. These results were also reflected in the PDT calculations - the 35

367 Hz and 45 Hz cultures had longer time to achieving PDT (Fig. 8B).

368 ***Morphology of ASCs after adipogenic differentiation***

369 Microscopic analysis of adipocytes that originated from hASCs revealed that the 25 Hz

370 vibrations mostly enhanced the adipogenic differentiation in comparison to the other groups (Fig.

371 9I, Panel B). The findings from gene expression analysis showed noticeable increase

372 of PPAR-γ and adiponectin (ADIQ) (Fig. 9A, B, Panel A) in 25 and 35 Hz stimulated groups

373 compared to control. However, qRT-PCR findings also showed similar gene expression of leptin

374 (LEP) (Fig. 9C, Panel A). The adipocytes derived from 25 Hz stimulated group were highly

375 abundant with large lipid vacuoles, positively stained by Oil Red O staining, and absorbed the

376 highest percentage of dye (Fig. 10A). The smallest adipocyte diameter was observed in the

377 control group (ranges between 60 and 92 um), while adipocytes treated with 35Hz were

378 characterized by the highest average size (ranges between 90 and 119 um) (Fig. 10B).

379

380

381   **Discussion**

382   Cartilage defects, especially in cases of osteoarthritis, have a serious impact on the patient's

383   quality-of-life and functionality. The increasing prevalence of degenerative joint diseases is

384   explained by the increasing life expectancy of the general population [42]. Tissue-engineering

385   approaches including the application of externally applied signals such as stimulation with

386   electric currents [43, 44], laser [45], or ultrasound vibration [46, 47], are promising tools for

387   overcoming this problem. However, these methods also have several shortcomings, such as

388   emission of high temperature or generation of rarefactional pressure, which may lead to mild

389   heating, coagulative necrosis, tissue vaporization or inducing pulsation of pre-existing gas bodies

390   [48].

391   Even more promising is the combination of MSCs therapy with innovative devices that are able

392   to induce particular external signals, which enhance the regeneration of injured tissues. Since

393   stem cells viability, proliferation status, and differentiation potential are widely connected with

394   their regenerative potential [49, 50], searching for external stimulating factors that may enhance

395   the mentioned MSCs features, before clinical application seems to be a crucial factor, when

396   MSCs for cartilage regeneration purposes are considered. Furthermore, effective external

397   stimulation may help overcome the age-related decrease in chondrogenic differentiation potential

398   of hASCs that currently poses a limitation to their clinical application in cell-based therapies

399   [14]. Therefore, in the current study, we hypothesized that LMLF may enhance the chondrogenic

400   differentiation potential of hASCs and simultaneously alter the differentiation toward fat tissue.

401   We found that when the PF of hASCs cultured in chondrogenic conditioned medium is

402   considered, both the 25 Hz and the 35 Hz vibration frequencies reduce the PF of hASCs.

403   Additionally, the PDT reached the highest level in cells treated with 25 Hz, which strongly

404   correlates with the obtained PF factor. As recently reported, the PDT of MSCs directly correlates

405   with their replicative senescence, which is linked to the decrease in the size of cell aggregation

406   [51]. In each experimental group, the PDT was higher in comparison with other studies [52].

407   This may be due to the fact that cells were rapidly differentiated into osteoblasts or adipocytes,

408   and that their proliferation activity was significantly reduced. Sepúlveda et al. [53] reported that

409   cell senescence abrogates the therapeutic potential of human mesenchymal stem cells in a lethal

410   endotoxemia model. Therefore, searching for methods that might improve the PDT level seems

411   to be crucial in the context of clinical application of MSCs. Interestingly, although hASCs

412   treated with 35 Hz had low PF and long PDT, they also developed the largest chondro nodules.

413   Furthermore, the highest concentration of absorbed Safranin O staining was observed in nodules

414   originating from cells treated with 35 Hz vibration. This likely demonstrates that 35 Hz

415   vibrations induce the highest synthesis of glycosaminoglycans (GAG), and thus indicates that the

416   chondrogenic process is highly efficient.

417   The GAGs have an unquestionable influence on biomechanical properties of cartilage. They

418   serve as an important component of extracellular matrix (ECM), which directly affects the

419   integrity of cartilage. Our data demonstrates that the 35 Hz vibration model could be applied to

420   stimulate chondrocytes, which originated from hASCs to produce ECM of high biomechanical

421   properties manifested by rich in collagen type II and proteoglycans. The most extensive

422   morphometrical properties, i.e. length and height of single nodules, were observed in 2D culture

423   cells that were treated with the 35Hz vibrations protocol. Slightly weaker chondro nodule

424   development, as well as cytoskeleton formation, was observed in the 2D culture treated with

425   25Hz vibrations in comparison to the others, as well as to the control group (Figure 4).

426   In order to determine which of the investigated frequencies has a more significant impact on the

427   process of chondrogenesis, we applied quantitative ELISA and qPCR in order to evaluate the

428   concentration of BMP-2 and the relationship between collagen type I and II in the culture

429   medium. We found in 3D culture treated with 35 Hz the highest concentrations of BMP-2

430   (Figure 5), and at the same time -collagen type II, in the 2D culture treated with 35 Hz (Figure

431   4). However, 25 Hz vibrations caused an increase in synthesis, albeit slightly smaller amounts of

432   investigated proteins. Our obtained results stand in good agreement with the findings of van

433   Cashion et al. [54], who reported that low frequency vibrations can induce secretion of BMP-2 in

434   human umbilical cord derived MSCs. It is worth noting that both the 25 Hz and 35 Hz vibration

435   stimulated chondrocytes originating from hASCs had elevated synthesis of type II rather than

436   type I collagen. It is well known that elasticity of articular cartilage is dependent on the proper

437   relationship between synthesis and secretion of collagen types I and II. Simultaneously, we

438   observed, that 35Hz vibration stimuli in 2D culture caused up-regulation of sex-determining

439   region Y protein (SRY)-box 9 (SOX9) that is the primary regulator of chondrogenic

440   differentiation on an in vitro as well as an in vivo level. The observed up-regulation of Sox-9,

441   strongly corresponded with elevated expression of collagen type II, which is to be expected as

442   Sox-9 directly regulates expression of collagen gene (COLL II) in chondrogenic progenitor cells,

443   as well as chondrocytes [55, 56]. Moreover, SOX9 determines functions of RUNX2 and exerts a

444   dominant function over RUNX2 in mesenchymal precursors [57]. In this study, we confirmed

445   this effect; gene expression of SOX9 and RUNX2 are overlapped and enhanced in cells treated

446   with vibrations.

447   The positive effect of LFLM on the functional chondrogenic differentiation process might be

448   explained by up-regulation of the integrin family. Here, we found that both frequencies i.e. 25

449 and 35 Hz, affect up-regulation of integrin α3, α4, β1 and β3 subunits on the mRNA level,

450 although statistical significance was observed only in 35Hz stimulated cells. Furthermore, β1

451 integrin has been shown to play a crucial role in attachment and survival of MSCs during the

452 chondrogenesis process. Furthermore, we observed that LFLM, in general, significantly down

453 regulates integrin α5β5 expression. Moreover, we observed down-regulation of α5 integrins of

454 MSCs stimulated with all tested frequencies. Thus our results stand in good agreement with

455 Martino and colleagues (2008), that showed involvement of α5 integrins more in osteogenic

456 rather than chondrogenic differentiation process [58].

457 Finally, the effect of vibration loading with particular frequencies on the adipogenic

458 differentiation potential of hASCs was investigated. We found that among all tested frequencies,

459 35 Hz significantly inhibited adipogenesis in hASCs. The obtained results stand in good

460 agreement with the findings by Oh at al. [59] who reported that 20 and 30 Hz sub-sonic

461 vibrations inhibited the proliferation of 3T3-L1 preadipocytes, Additionally, we observed the

462 smallest absorption of Oil red O staining when cells were treated with 35 Hz vibration, However

463 we observed increased number of lipid droplets in 25 Hz vibration group, but the observed

464 changes were only on a morphological level. In adipogenic gene expression level of we did not

465 observed significant changes between 25 Hz and other investigated groups.

466

468 **Conclusions**

469 In conclusion, the vibration-loading device designed for the purpose of this study successfully

470 generated controlled vibrational forces to hASCs cultured on 24-well, as well as 3D pelleted

471 cells model. Our results indicate that LFLM vibrations differently act on both chondrogenic, as

472 well as adipogenic potential of hASCs. The most important finding of this study suggests that 35

473 Hz frequency vibrations enhance chondrogenic potential of hASCs with simultaneous inhibition

474 of hASCs differentiation toward adipocytes. Finally, we conclude that mechanical signals,

475 especially 35 Hz frequency vibrations might be potentially used in construction of therapeutic

476 devices which may prove useful in the field of articular degenerative diseases treatment.

477

478 **Acknowledgments**

479 We thank Marta Jeleń for assistance during in vitro work and cell vibration generator prototype

480 preparation.

482 **References**

483   1. Chung C, and Burdick JA (2008). Engineering cartilage tissue. Advanced drug delivery
484   reviews, 60(2), 243-262.

485   2. Lin J, Zhang W, Jones A and Doherty M (2004). Efficacy of topical non-steroidal anti-
486   inflammatory drugs in the treatment of osteoarthritis: meta-analysis of randomised controlled
487   trials. bmj, 329(7461), 324.

488   3. Brandt KD: Effects of nonsteroidal anti-inflammatory drugs on chondrocyte metabolism in
489   vitro and in vivo. Am J Med. 1987, 83(5A): 29–34.

490   4. Iyer SS, Rojas M: Anti-inflammatory effects of mesenchymal stem cells: novel concept for
491   future therapies. Expert Opin. Biol. Ther. 2008, 8(5): 569-581.

492   5. Zuk PA, Zhu M, Mizuno H, Huang J, Futrell JW, Katz AJ, Benhaim P, Lorenz HP, Hedrick
493   MH. (2001) Multilineage cells from human adipose tissue: implications for cell-based
494   therapies. Tissue Eng. 7, 211–228.

495   6. Baer PC, Geiger H (2012) Adipose-derived mesenchymal stromal/stem cells: tissue
496   localization, characterization, and heterogeneity. Stem cells 2012, doi:10.1155/2012/812693

497   7. Marędziak M, Marycz K, Lewandowski D, Siudzinska A, Śmieszek A. (2015) Static
498   magnetic field enhances synthesis and secretion of membrane-derived microvesicles (MVs)
499   rich in VEGF and BMP-2 in equine adipose-derived stromal cells (EqASCs)-a new approach
500   in veterinary regenerative medicine. In Vitro Cellular & Developmental Biology. Animal.
501   51(3): 230–240.

502   8. Collino F, Deregibus MC, Bruno S, Sterpone L, Aghemo G, Viltono L, Camussi G (2010)
503   Microvesicles derived from adult human bone marrow and tissue specific mesenchymal stem
504   cells shuttle selected pattern of miRNAs. PloS one, 5(7), e11803.

505 9. Tetta C, Consiglio AL, Bruno S, Tetta E, Gatti E, Dobreva M, Cremonesi F, Camussi G

506   (2012) The role of microvesicles derived from mesenchymal stem cells in tissue

507   regeneration; a dream for tendon repair? Muscles Ligaments Tendons J. 2(3): 212–221.

508 10. Marycz K, Grzesiak J, Wrzeszcz K, Golonka P. (2012) Adipose stem cell combined with

509   plasma-based implant bone tissue differentiation in vitro and in a horse with a phalanx

510   digitalis distalis fracture: a case report. Veterinarni Medicina 57(11): 610–617; 2012.

511 11. Marycz K, Toker NY, Grzesiak J, Wrzeszcz K, Golonka P. (2012) The therapeutic effect of

512   autogenic adipose derived stem cells combined with autogenic platelet rich plasma in tendons

513   disorders hi horses in vitro and in vivo research. Journal of Animal and Veterinary Advances

514   11(23): 4324–4331; 2012.

515 12. Brittberg M, Lindahl A, Nilsson A, Ohlsson C, Isaksson O, Peterson L. Treatment of deep

516   cartilage defects in the knee with autologous chondrocyte transplantation. N Engl J Med

517   1994; 331: 889–895.

518 13. Nicpoń J, Marycz K, Grzesiak J, Śmieszek A, Toker ZY (2014). The advantages of autologus

519   adipose derived mesenchymal stem cells (AdMSCs) over the non-steroidal anti-inflammatory

520   drugs (NSAIDs) application for degenerative elbow joint disease treatment in dogs-Twelve

521   cases. Kafkas Univ Vet Fak Derg, 20(3), 345-350.

522 14. Choudhery MS, Badowski M, Muise A, Pierce J, Harris DT. Donor age negatively impacts

523   adipose tissue-derived mesenchymal stem cell expansion and differentiation. J Transl Med.

524   2014;12:8.

525 15. Marędziak M, Marycz K, Śmieszek A, Lewandowski D, Nezir Yaşar Toker (2014) The

526   influence of static magnetic fields on canine and equine mesenchymal stem cells derived

527   from adipose tissue. In Vitro Cell.Dev.Biol. – Animal, 50:562–571.

528   16. Hammerick KE, James AW, Huang Z, Prinz FB, Longaker MT. (2009) Pulsed direct current

529   electric fields enhance osteogenesis in adipose-derived stromal cells. Tissue Engineering Part

530   A, 16(3), 917-931.

531   17. Simmons CA, Matlis S, Thornton AJ, Chen S, Wang CY, Mooney DJ. (2003). Cyclic strain

532   enhances matrix mineralization by adult human mesenchymal stem cells via the extracellular

533   signal-regulated kinase (ERK1/2) signaling pathway. Journal of biomechanics, 36(8), 1087-

534   1096.

535   18. Lau E, Al-Dujaili S, Guenther A, Liu D, Wang L, You L (2010). Effect of low-magnitude,

536   high-frequency vibration on osteocytes in the regulation of osteoclasts. Bone, 46(6):1508-15.

537   19. Nikander, R Kannus P, Dastidar P, Hannula M, Harrison L, Cervinka T, Narra NG, Aktour

538   R, Arola T, Eskola H, Soimakallio S, Heinonen A, Hyttinen J, Sievänen H. (2009) Targeted

539   exercises against hip fragility. Osteoporos. Int. 20, 1321–1328.

540   20. Tirkkonen L, Halonen H, Hyttinen J, Kuokkanen H, Sievänen H, Koivisto AM, Haimi S

541   (2011). The effects of vibration loading on adipose stem cell number, viability and

542   differentiation towards bone-forming cells. Journal of The Royal Society Interface, 8(65),

543   1736-1747.

544   21. Luu YK, Capilla E, Rosen CJ, Gilsanz V, Pessin JE, Judex S, Rubin CT. (2009) Mechanical

545   stimulation of mesenchymal stem cell proliferation and differentiation promotes osteogenesis

546   while preventing dietary-induced obesity. J. Bone Miner. Res. 24, 50–61.

547   22. Edwards JH, Reilly GC (2015) Vibration stimuli and the differentiation of musculoskeletal

548   progenitor cells: Review of results in vitro and in vivo. World J Stem Cells. 7(3): 568–582.

549   23. Uzer G, Thompson WR, Sen B, Xie Z, Yen SS, Miller S, Bas G, Styner M, Rubin CT, Judex

550   S, Burridge K, Rubin J. (2015) Cell Mechanosensitivity to Extremely Low-Magnitude

551   Signals Is Enabled by a LINCed Nucleus. Stem Cells 33(6):2063-76.

552   24. Sen B, Xie Z, Case N, Styner M, Rubin CT, Rubin J. (2011) Mechanical signal influence on

553   mesenchymal stem cell fate is enhanced by incorporation of refractory periods into the

554   loading regimen. J Biomech. 44(4): 593-9.

555   25. Prè D, Ceccarelli G, Visai L, Benedetti L, Imbriani M, Cusella De Angelis MG, Magenes G

556   (2013) High-Frequency Vibration Treatment of Human Bone Marrow Stromal Cells

557   Increases Differentiation toward Bone Tissue. Bone Marrow Res. 2013: 803450.

558   26. Uzer G, Pongkitwitoon S, Ete Chan M, Judex S. (2013). Vibration induced osteogenic

559   commitment of mesenchymal stem cells is enhanced by cytoskeletal remodeling but not fluid

560   shear. J Biomech. 2013;46:2296–2302.

561   27. Popov C, Burggraf M, Kreja L, Ignatius A, Schieker M Docheva D. (2015). Mechanical

562   stimulation of human tendon stem/progenitor cells results in upregulation of matrix proteins,

563   integrins and MMPs, and activation of p38 and ERK1/2 kinases

564   28. Goessler UR, Bugert P, Bieback K, Stern-Straeter J, Bran G, Sadick H, Hörmann K, Riedel

565   F. In vitro analysis of integrin expression in stem cells from bone marrow and cord blood

566   during chondrogenic differentiation. J Cell Mol Med. 2009;13(6):1175-84.

567   29. Hering TM. Regulation of chondrocyte gene expression. Front Biosci. 1999;4:D743-61.

568   30. Hynes RO. Integrins: versatility, modulation, and signaling in cell adhesion. Cell.

569   1992;69(1):11-25.

570   31. Giancotti FG, Ruoslahti E. Integrin signaling. Science. 1999;285(5430):1028-32.

571   32. Albelda SM, Buck CA. Integrins and other cell adhesion molecules. FASEB J.

572   1990;4(11):2868-80.

573   33. Salter DM, Hughes DE, Simpson R, Gardner DL. Integrin expression by human articular

574   chondrocytes. Br J Rheumatol. 1992;31(4):231-4.

575   34. Lee J BC, W, Qi WN, Scully SP. The involvement of beta1 integrin in the modulation by

576   collagen of chondrocyte-response to transforming growth factor-beta1. J Orthop Res.

577   2002;20(1):66-75.

578   35. Xie, L., Rubin, C. and Judex, S. (2008). Enhancement of the adolescent murine

579   musculoskeletal system using low-level mechanical vibrations. J. Appl. Physiol. 104, 1056–

580   1062.

581   36. Wehrle E, Liedert A, Heilmann A, Wehner T, Bindl R, Fischer L, Haffner-Luntzer M, Jakob

582   F, Schinke T, Amling M, Ignatius A (2015) The impact of low-magnitude high-frequency

583   vibration on fracture healing is profoundly influenced by the oestrogen status in mice. Dis

584   Model Mech. 8(1):93-104.

585   37. Rubin C, Judex S, Qin YX. (2006) Low-level mechanical signals and their potential as a non-

586   pharmacological intervention for osteoporosis. Age Ageing 35, 32.

587   38. Grzesiak J, Marycz K, Czogala J, Wrzeszcz K, Nicpon J (2011) Comparison of behavior,

588   morphology and morphometry of equine and canine adipose derived mesenchymal stem cells

589   in culture. Int J Morphol 29: 1012–1017.

590   39. Marycz K, Smieszek A, Grzesiak J, Donesz-Sikorska A, Krzak-Ros J (2013) Application of

591   bone marrow and adipose-derived mesenchymal stem cells for testing the biocompatibility of

592   metal-based biomaterials functionalized with ascorbic acid. Biomed Mater 8: 065004.

593   40. Chomczynski P, Sacchi N (1987) Single-step method for RNA isolation by acid guanidinium

594   thiocyanate-phenol-chloroform extraction. Anal Biochem 162: 156-159.

595   41. Kim HJ, Im GI. The effects of ERK1/2 inhibitor on the chondrogenesis of bone marrow- and

596   adipose tissue-derived multipotent mesenchymal stromal cells. Tissue Eng Part A

597   2010;16(3):851e60.

598   42. Raeissadat S, Rayegani S, Babaee M, Ghorbani E (2013): The Effect of Platelet-Rich Plasma

599   on Pain, Function, and Quality of Life of Patients with Knee Osteoarthritis, Pain Res Treat.

600   2013; 2013: 165967.

601   43. Ciombor DM, Aaron RK. (2005) The role of electrical stimulation in bone repair. Foot Ankle

602   Clin; 10:579–593, vii.

603   44. Foley KT, Mroz TE, Arnold PM, Chandler HC Jr, Dixon RA, Girasole GJ, Renkens KL Jr,

604   Riew KD, Sasso RC, Smith RC, Tung H, Wecht DA, Whiting DM. Randomized,

605   prospective, and controlled clinical trial of pulsed electromagnetic field stimulation for

606   cervical fusion. Spine J. 2008;8:436–442.

607   45. Miloro M, Miller JJ, Stoner JA. Low-level laser effect on mandibular distraction

608   osteogenesis. J Oral Maxillofac Surg. 2007;65:168–176.

609   46. El-Mowafi H, Mohsen M. The effect of low-intensity pulsed ultrasound on callus maturation

610   in tibial distraction osteogenesis. Int Orthop. 2005;29:121–124.

611   47. Taylor KF, Rafiee B, Tis JE, Inoue N. (2007) Low-intensity pulsed ultrasound does not

612   enhance distraction callus in a rabbit model. Clin Orthop Relat Res;459:237–245.

613   48. Miller D, Smith N, Bailey M, Czarnota G, Hynynen K, Makin I, and American Institute of

614   Ultrasound in Medicine Bioeffects Committee (2012): Overview of Therapeutic Ultrasound

615   Applications and Safety Considerations, J Ultrasound Med.; 31(4): 623–634.

616   49. Krampera M, Pasini A, Pizzolo G, Cosmi L, Romagnani S, Annunziato F (2006):

617   Regenerative and immunomodulatory potential of mesenchymal stem cells; Current Opinion

618   in Pharmacology, Volume 6, Issue 4, August 2006, Pages 435–441.

619 50. Mishra A, Tummala P, King A, Lee B, Kraus M, Tse V, Jacobs CR (2009): Buffered

620   Platelet-Rich Plasma Enhances Mesenchymal Stem Cell Proliferation and Chondrogenic

621   Differentiation Tissue Engineering Part C: Methods, Vol. 15, No. 3: 431-435

622 51. Yoon IS, Chung CW, Sung JH, Cho HJ, Kim JS, Shim WS, Shim CK, Chung SJ, Kim DD.

623   Proliferation and chondrogenic differentiation of human adipose-derived mesenchymal stem

624   cells in porous hyaluronic acid scaffold. J Biosci Bioeng. 2011 Oct;112(4):402-8.

625 52. Hass, R., Kasper, C., Bohm, S., & Jacobs, R. (2011). Different populations and sources of

626   human mesenchymal stem cells (MSC): a comparison of adult and neonatal tissue-derived

627   MSC. Cell Commun Signal, 9(1), 12.

628 53. Sepúlveda JC, Tomé M, Fernández ME, Delgado M, Campisi J, Bernad A, González MA

629   (2014). Cell senescence abrogates the therapeutic potential of human mesenchymal stem

630   cells in the lethal endotoxemia model. Stem Cells.

631 54. Cashion A, Caballero M, Halevi A, Pappa A, Dennis RG, van Aalst JA (2014):

632   Programmable Mechanobioreactor for Exploration of the Effects of Periodic Vibratory

633   Stimulus on Mesenchymal Stem Cell Differentiation, BioResearch Open Access, Volume 3,

634   Number 1.

635 55. Akiyama H. Control of chondrogenesis by the transcription factor Sox9. Mod. Rheumatol.

636   2008;18, 213–219

637 56. Bell DM, Leung KK, Wheatley SC, Ng LJ, Zhou S, Ling KW, Sham MH, Koopman P, Tam

638   PP, Cheah KS. SOX9 directly regulates the type-II collagen gene. Nat Genet.

639   1997;16(2):174-8.

640   57. Zhou G, Zheng Q, Engin F, Munivez E, Chen Y, Sebald E, Krakow D, Lee B. (2006)

641   Dominance of SOX9 function over RUNX2 during skeletogenesis. Proc Natl Acad Sci U S

642   A. 103(50):19004-9.

643   58. Martino MM, Mochizuki M, Rothenfluh DA, Rempel SA, Hubbell JA, Barker TH.

644   Controlling integrin specificity and stem cell differentiation in 2D and 3D environments

645   through regulation of fibronectin domain stability. Biomaterials. 2009;30(6):1089-97.

646   59. Oh ES, Seo YK, Yoon HH, Cho H, Yoon MY, Park JK (2011): Effects of sub-sonic vibration

647   on the proliferation and maturation of 3T3-L1 cells. Life Sci, Jan 17;88(3-4):169-77

648

649

650
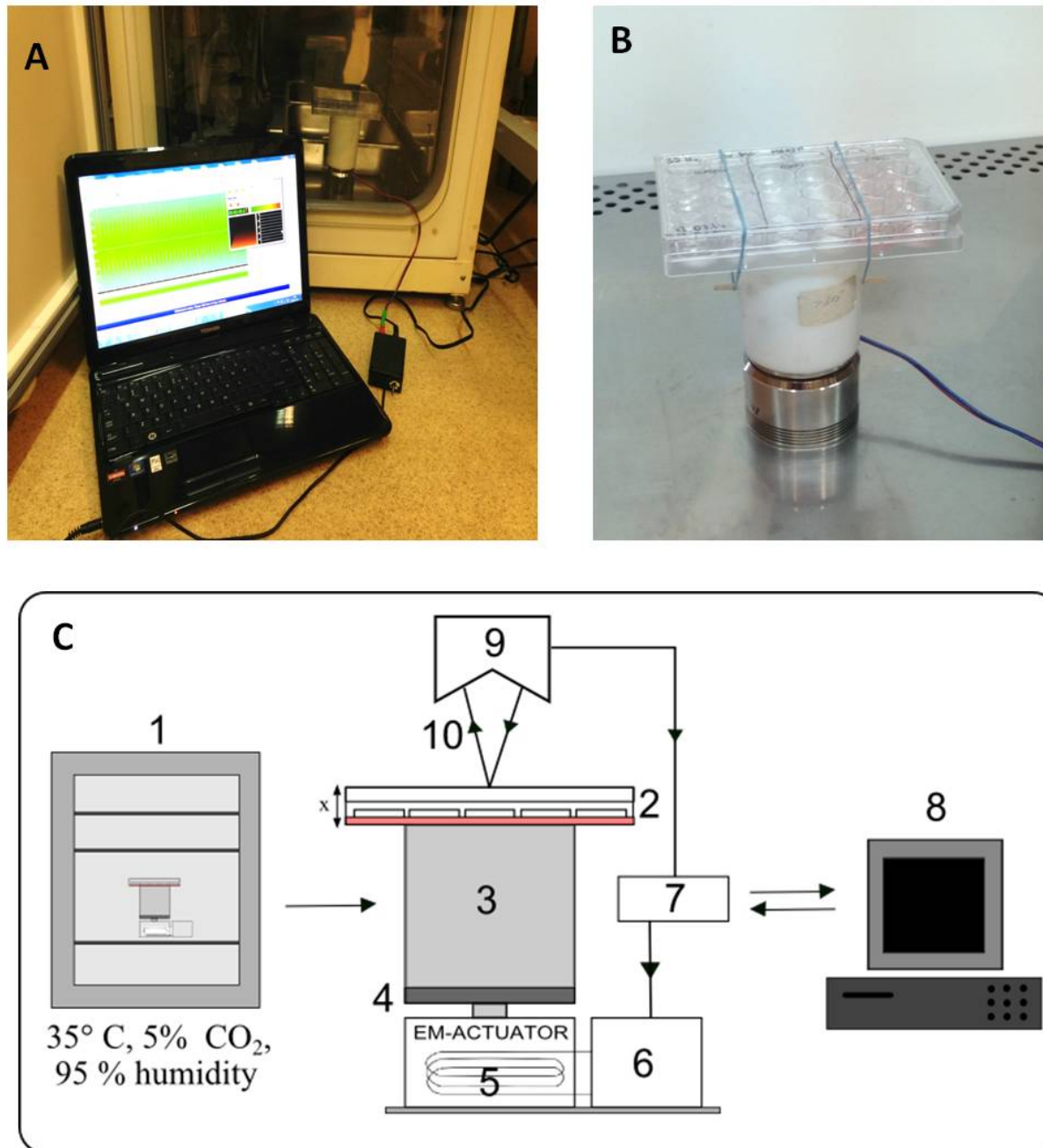
Figure 1. Cell vibration generator prototype. Acutator with cell culture plate connected with PC software, put inside a CO_2 incubator (A). Cell culture plate attatched to the spacer under electro-magnetic acutator (B). Connection diagram and flow of signals during vibration stimulation. The electromagnetic actuator was supplied directly by the amplifier. The displacement signal waveform was generated in the computer software and sent through a digital-to-analog converter to the amplifier. 1 – incubator, 2 - 24-well culture plate, 3 – spacer, 4 – stiff movable plate, 5 – electro-magnetic actuator (EM-ACTUATOR) with coil inside, 6 – signal amplifier, 7 – measuring card with A/C

657   and C/A converters, 8 – PC and software, 9 – laser displacement sensor head, 10 – laser beam. x shows the

658   movement direction of the culture plate (C)

659
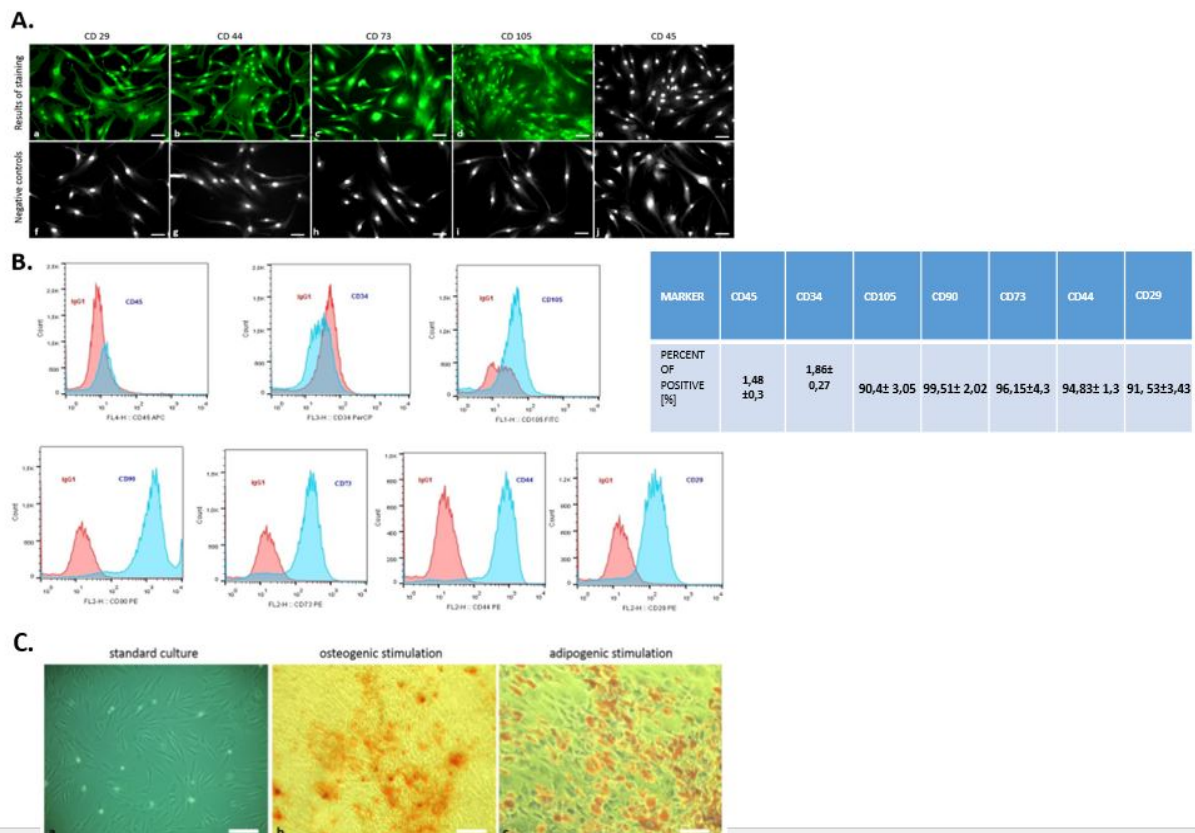
660   **Figure 2.** The expression of specific cell markers CD29, CD44, CD73 and CD105 and the lack of hematopoetic cell

661   marker CD45 (A). Characterization of hASCs FACS analysis. FACS histograms of passage 3 ASC simultaneously

662   stained for CD45, CD34, CD105, CD90, CD73, CD44, CD29, and IgG1 as negative control. Histograms are

663   representative of 3 independent flow cytometry analyses. Red histograms: IgG1 negative control; blue histograms:

664   antibody specific staining (B). Multipotency assay- standard culture and differentiated cultures after Alizarin Red

665   staining for osteogenic stimulation (mag. 50x, scale bar = 200 µm) and Oil Red O staining for adipogenic

666   stimulation (mag. 100x, scale bar = 400 µm) (C).

667

Chondrogenesis proliferation factor and population doubling time

668
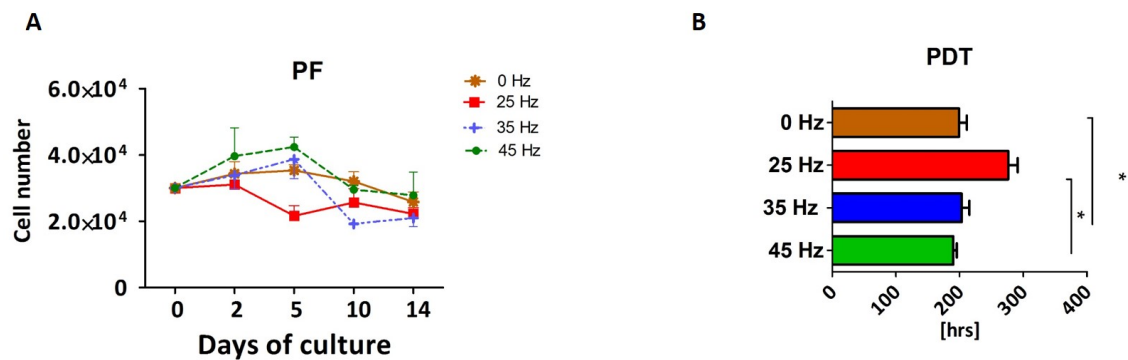
669   **Figure 3.** Proliferation factor (A) and population doubling time (PDT) (B) of hASCs treated with 0, 25, 35 and 45

670   Hz vibration frequencies during chondrogenic stimulation. * p-value < 0.05.

671

672
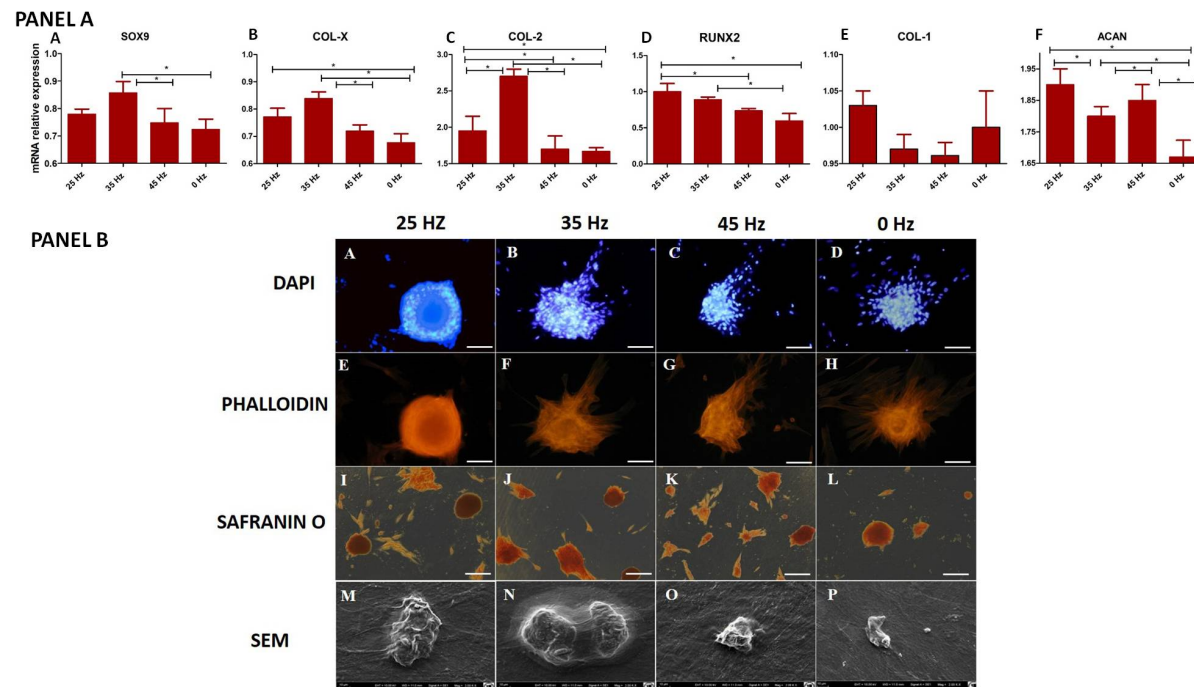
673 **Figure 4. Panel A** RT-qPCR for chondrogenesis genes: SOX9, COL-X, COL-2, RUNX2, COL-1 and ACAN from

674 hASCs that underwent chondrogenic induction on culture plates with treatment with 0, 25, 35, 45 Hz vibrations. * p-

675 value < 0.05 **Panel B** Cell morphology of chondroblasts originated from hASCs cultured on plates visualized by

676 fluorescence stainings (DAPI A-D and Phalloidin E-H), Safranin staining (I-L). Scale bars A-H 100 μm and I-L 200

677 μm and scanning electron microscope photographs (Mag. 2000x).

678

PANEL A

PANEL B

679
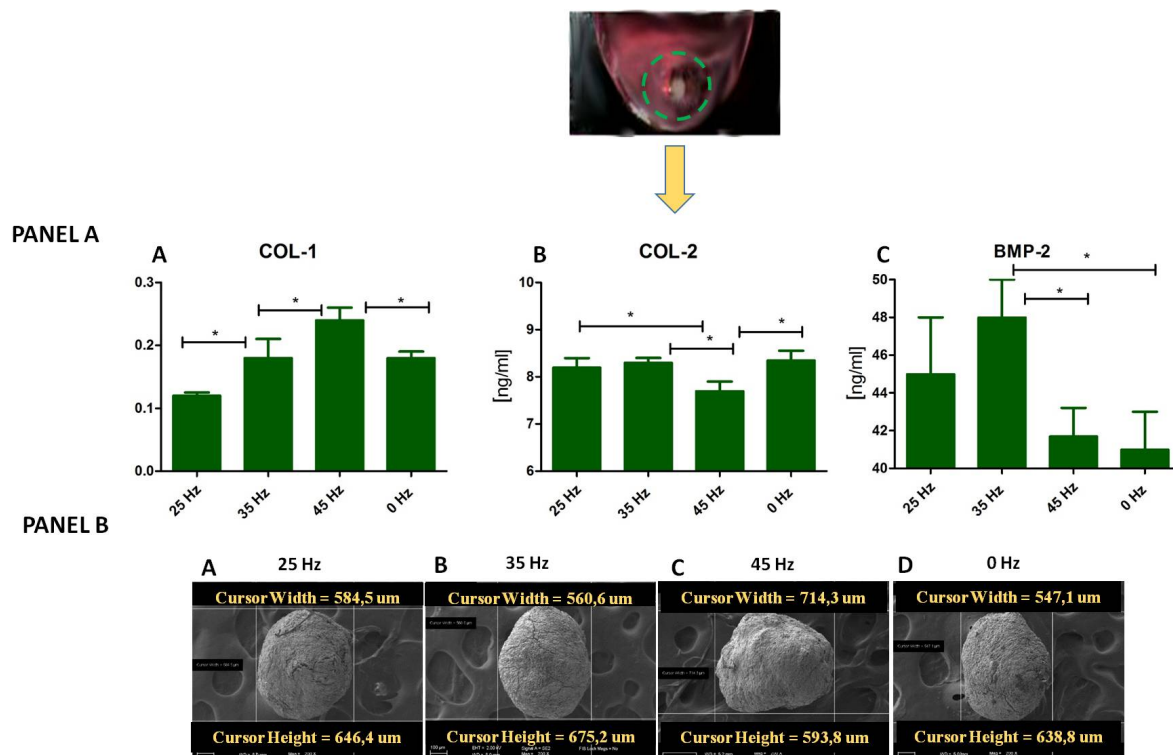
680   **Figure 5. Panel A** Comparison of Col-1 , Col-2 and BMP-2 levels by ELISA hASCs pellets after 14 days of

681   chondro-induction. **Panel B** Morphological characterization and comparison of chondro-nodules from cells cultured

682   at pellet.

683

A

B

684
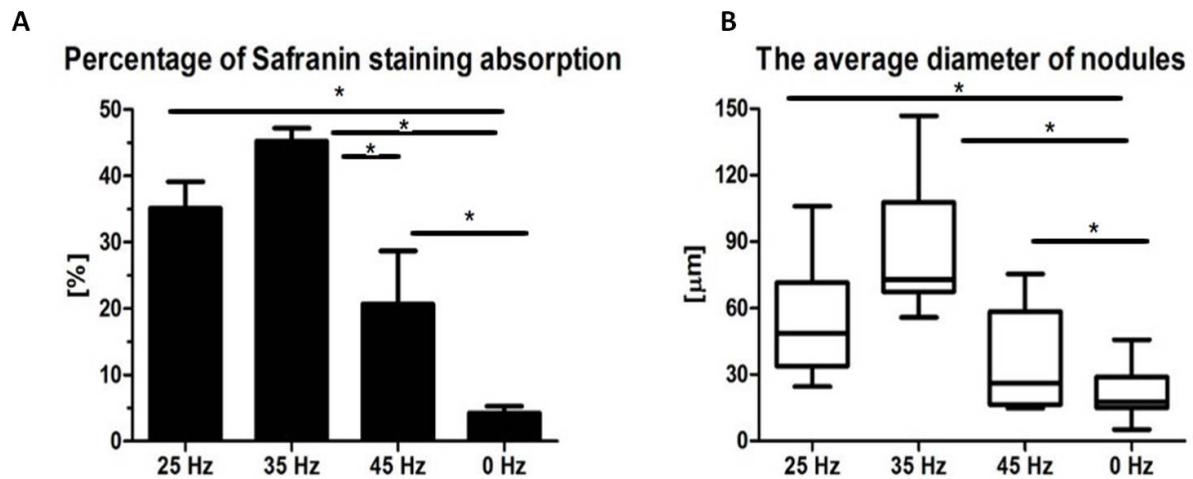
685   **Figure 6.** Percentage of Safranin staining absorption (A) and the average diameter of chondrogenic nodules (B)

686   from chondroblasts that originated from hASCs. * p-value < 0.05.

687

688
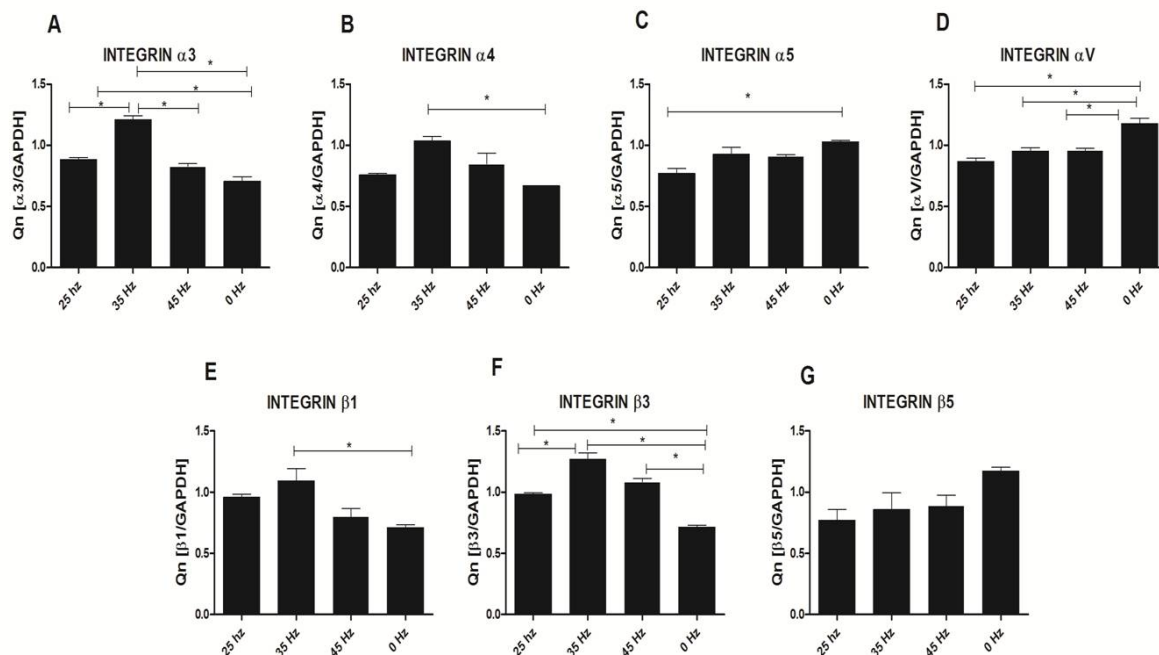
689   **Figure 7.** Integrin expression changes after mechanical stimulation of ASCs. Quantitative PCR analysis for integrin

690   alpha 3, 4, 5, V and beta 1, 3, 5 subunits. *p < 0.05.

691

692

693   **Figure 8.** Proliferation factor (A) and population doubling time (PDT) (B) of hASCs treated with 0, 25, 35 and 45

694   Hz vibration frequencies during adipogenic stimulation. * p-value < 0.05.

695

PANEL A

PANEL B

696
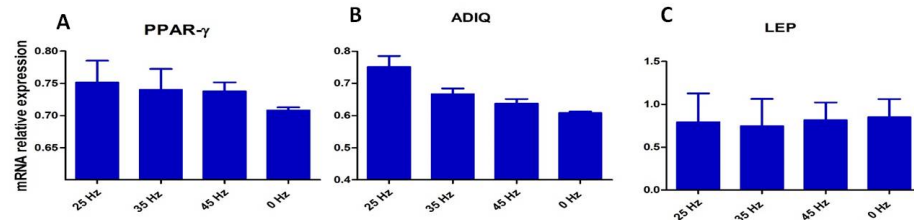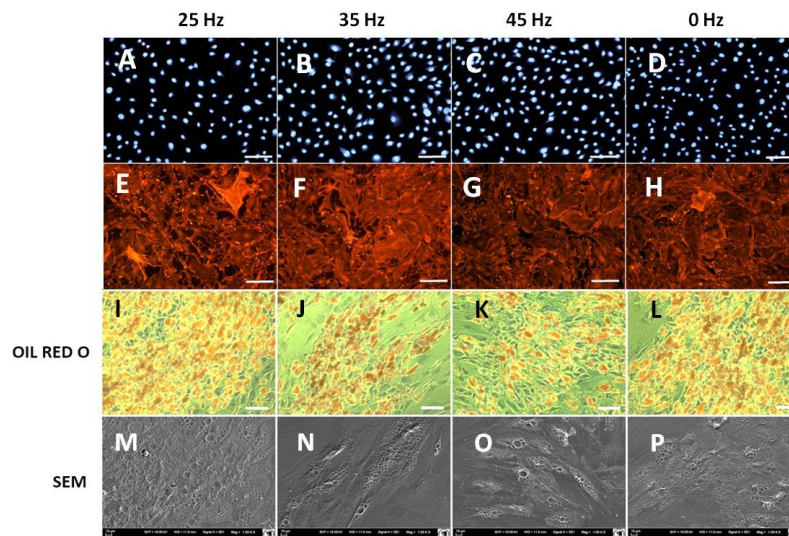
Figure 9. Panel A RT-qPCR for adipogenesis genes: PPAR-gamma, ADIQ, LEP from hASCs that underwent adipogenic induction on with treatment with 0, 25, 35, 45 Hz vibrations. * p-value < 0.05 **Panel B** Cell morphology of adipocytes originated from hASCs visualized using fluorescence stainings (Phalloidin, DAPI; Mag. 50x, scale bar 200 μm), Oil Red O Staining (100x, scale bar = 400 μm) and scanning electron microscope photographs (1000x).

701

702
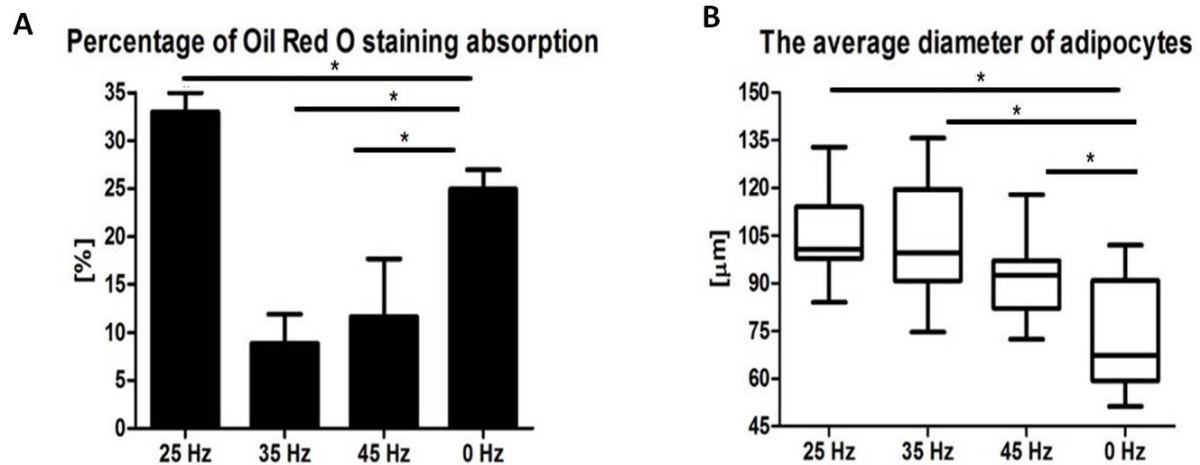
703 **Figure 10.** Percentage of Oil Red O staining (A) absorption and the average diameter (B) of adipocytes. * p-value <

704 0.05

705

706

Sequences of qPCR primers

Sequences of qPCR primers used for the amplification of human mRNA to chondrogenic genes

1 **Tables:**

Gene name	Primer sequentions	Ann. T, °C	Accession number
GAPDH	Forward 5'- GTCAGTGGTGGACCTGACCT -3' Reverse 5'- CACCACCCTGTTGCTGTAGC -3'	60	NM_002046
Collagen type I (COL1A1)	Forward 5'- GTGATGCTGGTCCTGTTGGT -3' Reverse 5'- CACCATCGTGAGCCTTCTCT -3'	60	NM_000088.3
Collagen type II (COL2A1)	Forward 5'- GACAATCTGGCTCCCAAC -3' Reverse 5'- ACAGTCTTGCCCCACTTAC -3'	60	NM_001844.4
Aggrecan (ACAN)	Forward 5'- GCCTACGAAGCAGGCTATGA -3' Reverse 5'- GCACGCCATAGGTCCTGA -3'	60	NM_013227.3
SOX-9	Forward 5'-AGCGAACGCACATCAAGAC-3' Reverse 5'- GCTGTAGTGTGGGAGGTTGAA-3'	65	NM_000346
RUNX-2	Forward 5'- GTGATAAATTCAGAAGGGAGG-3' Reverse 5'- CTTTTGCTAATGCTTCGTGT-3'	65	NM_001024630
Collagen type X (Col-X)	Forward 5'-CAGTCATGCCTGAGGGTTTT-3' Reverse 5'-GGGTCATAATGCTGTTGCCT-3'	65	NM_000493
Adiponectin (ADIQ)	Forward 5'-AGGGTGAGAAAGGAGATCC-3' Reverse 5'- GGCATGTTGGGGATAGTAA-3'	60	XM_011513324.1
Leptin (LEP)	Forward 5'- ATGACACCAAAACCCTCATCAA-3' Reverse 5'- GAAGTCCAAACCGGTGACTTT-3'	60	XM_005250340.3
PPAR-gamma	Forward 5'- ATGACACCAAAACCCTCATCAA- 3' Reverse 5'- GAGCGGGTGAAGACTCATGTCTGTC-3'	60	AB565476.1
Integrin α3	Forward 5'-ATCTTGAGAGCCACAGTCA-3' Reverse 5'-cTGGGTCCTTCTTTCTAGTTC-3'	52	(NM_002204)
Integrin α4	Forward 5'-AATGGATGAGACTTCAGCACT-3' Reverse 5'-CTCTTCTGTTTTCTTCTTGTAGG-3'	58	(NM_000885)
Integrin α5	Forward 5'-ACTAGGAAATCCATTCACAGTTC-3' Reverse 5'-GCATAGTTAGTGTTCTTTGTTGG-3'	52	(NM_002205)

Integrin αv	Forward 5′-GGAGCACATTTAGTTGAGGTAT -3′ Reverse 5′-ACTGTTGCTAGGTGGTAAAACT-3′	56	(NM_002210)
Integrin β3	Forward 5′-CTGCTGTAGACATTTGCTATGA-3′ Reverse 5′-GCCAAGAGGTAGAAGGTAAATA-3′	52	(NM_000212)
Integrin β5	Forward 5′-CTGTGGACTGATGTTTCCTT-3′ Reverse 5′-GTATGCTGGTTTTACAGACTCC-3′	54	(NM_002213)
Integrin β5	Forward 5′- GAAGGGTTGCCCTCCAGA -3' Reverse 5′- GCTTGAGCTTCTCTGCTGTT-3'	60	NM_002211.3

2 **Table 1**. Sequences of qPCR primers used for the amplification of human mRNA to chondrogenic genes.

Vibration generation prototype
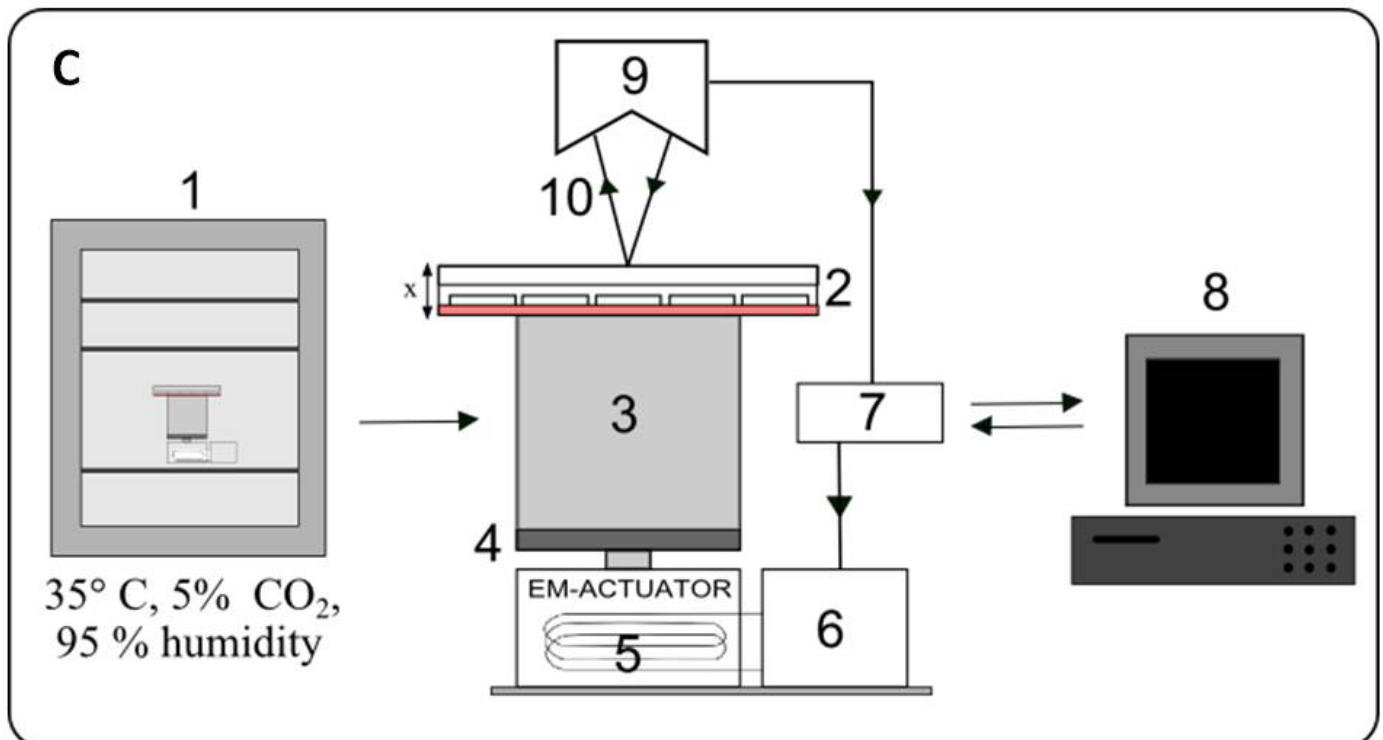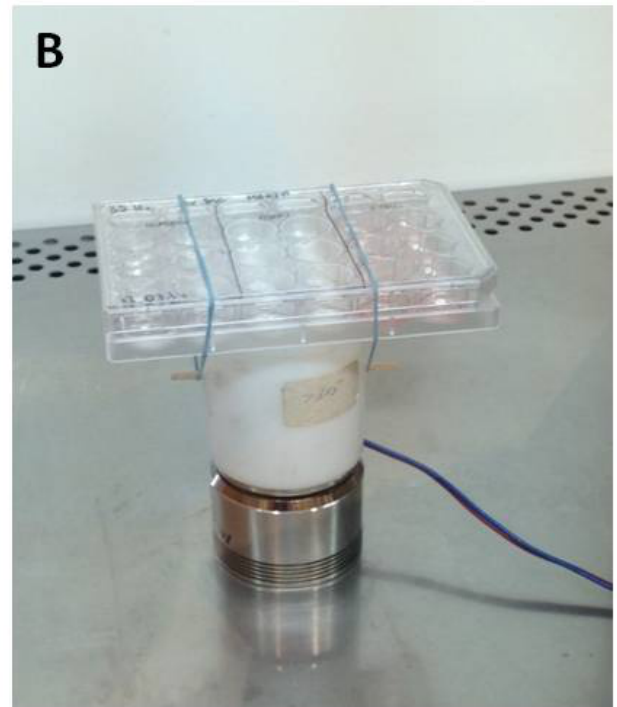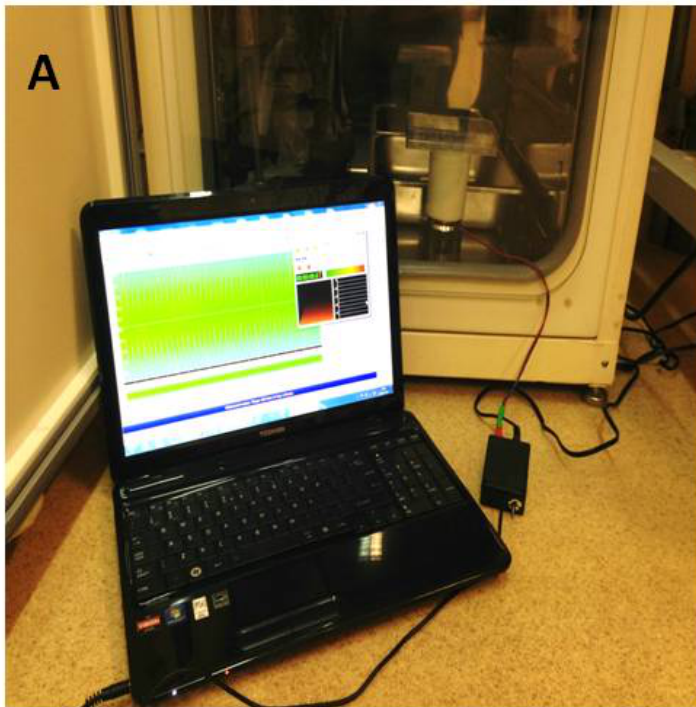
2

Phenotyping and multipotency test

3
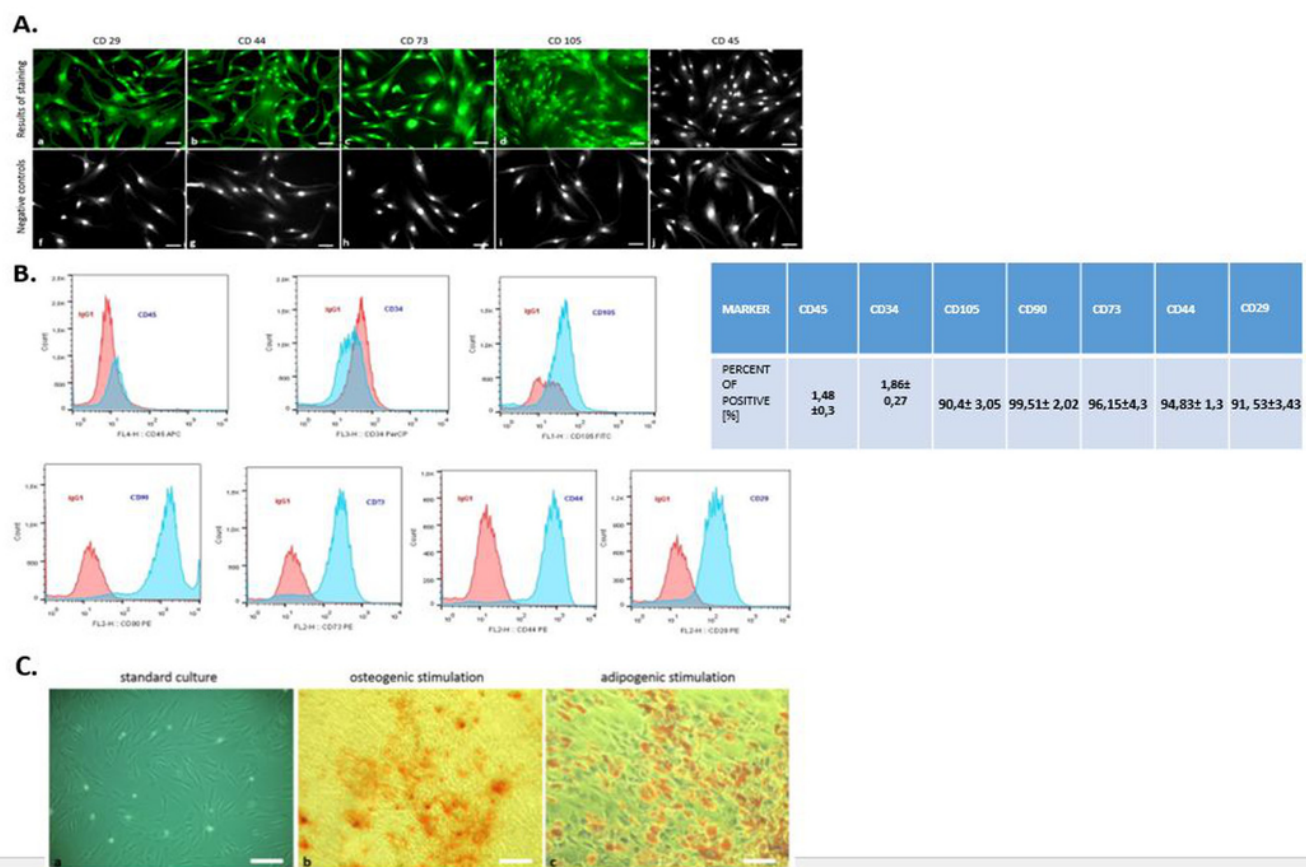
proliferation factor and PDT chondrogenesis
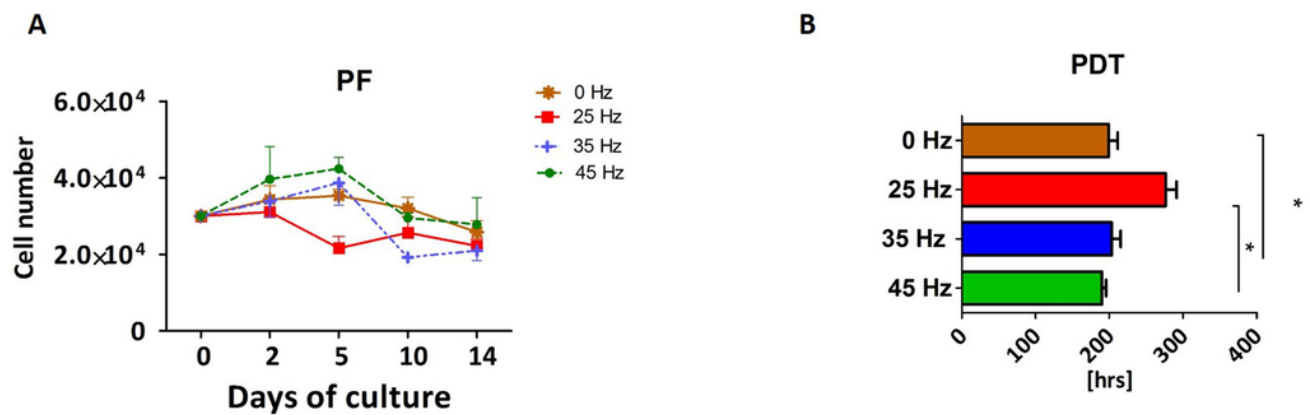
qPCR and morphology chondroblasts
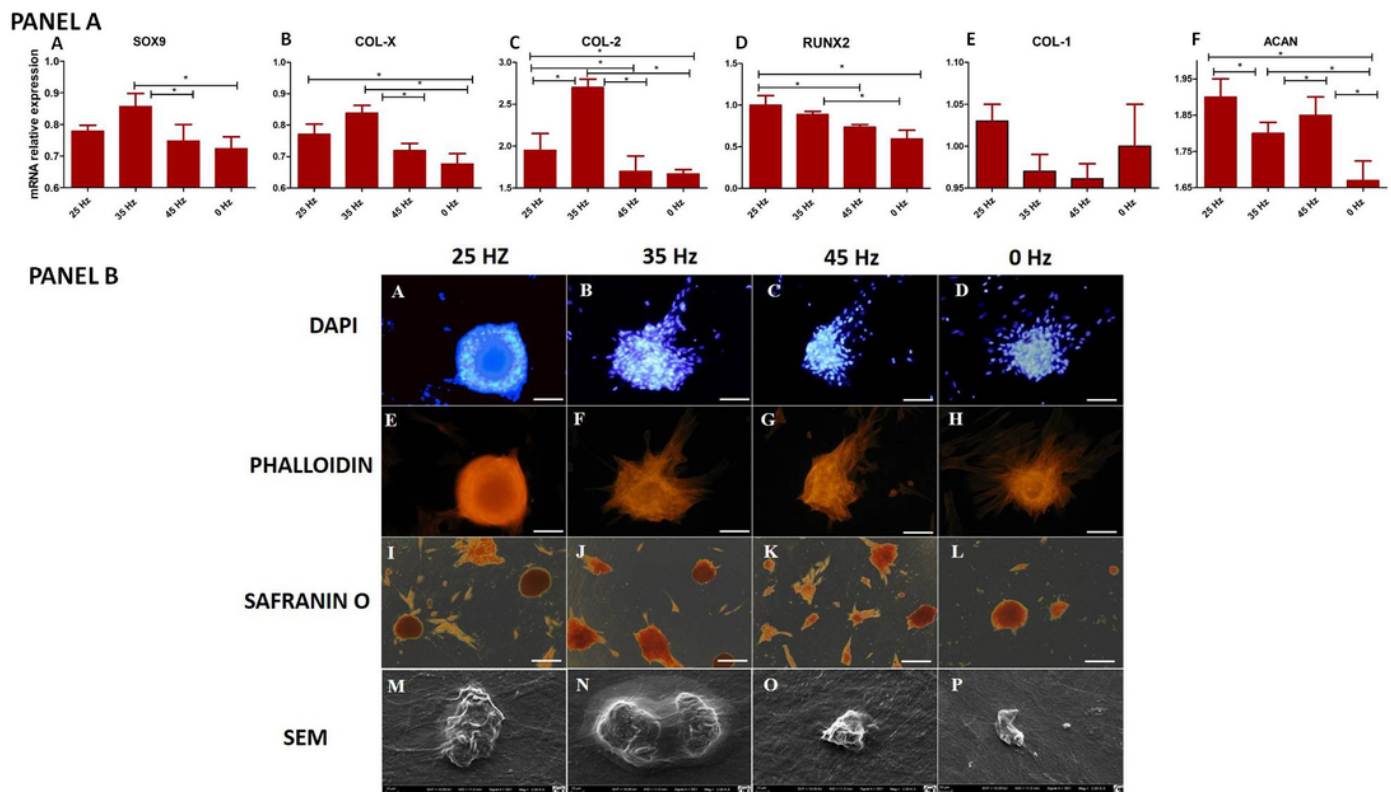
ELISA and chondro nodules

PANEL A

A COL-1

B COL-2

C BMP-2

PANEL B

A 25 Hz | B 35 Hz | C 45 Hz | D 0 Hz

Cursor Width = 584,5 um | Cursor Width = 560,6 um | Cursor Width = 714,3 um | Cursor Width = 547,1 um

Cursor Height = 646,4 um | Cursor Height = 675,2 um | Cursor Height = 593,8 um | Cursor Height = 638,8 um
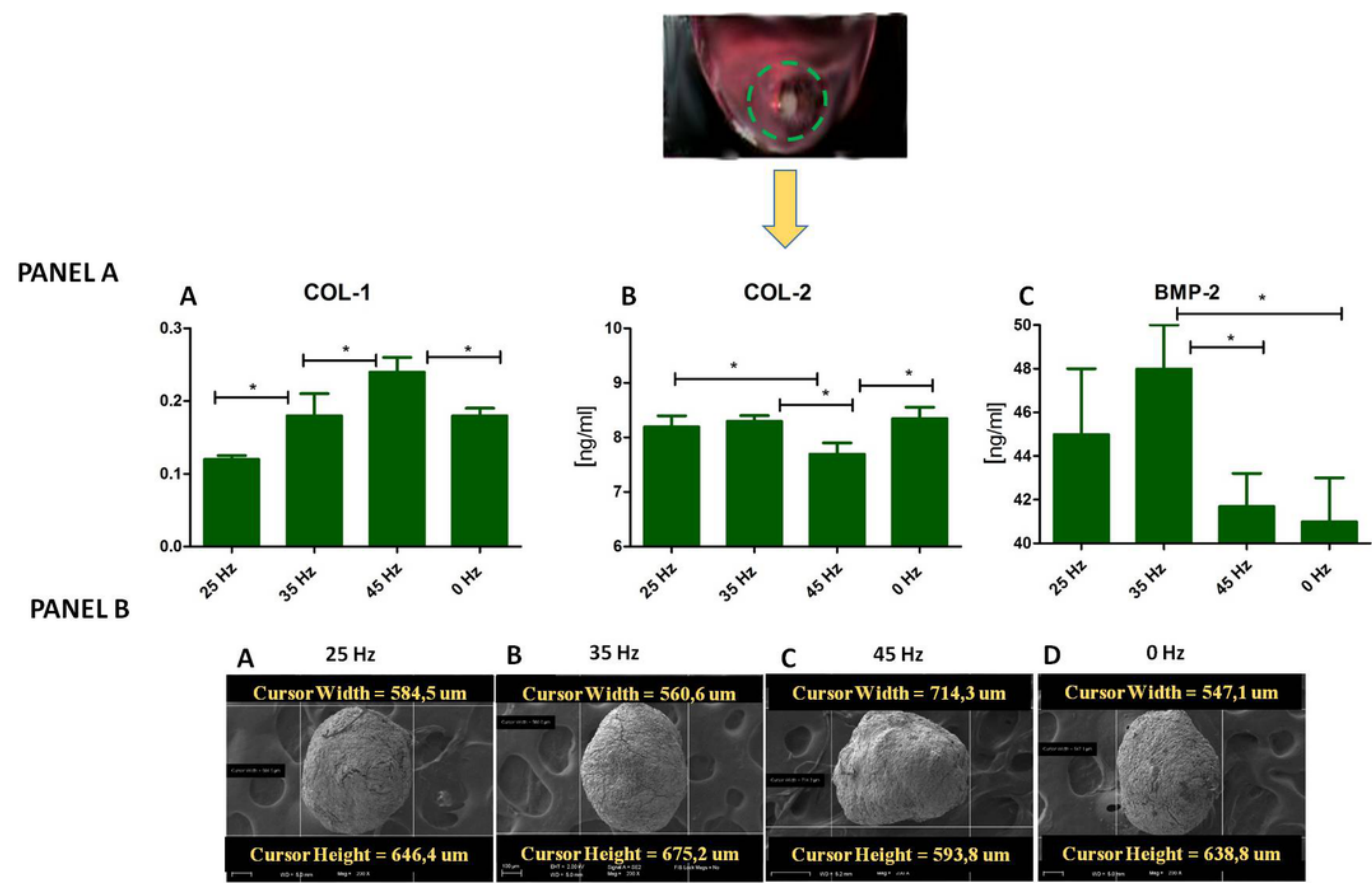
safranin absorbtion and diametres of chondronodules

A

B
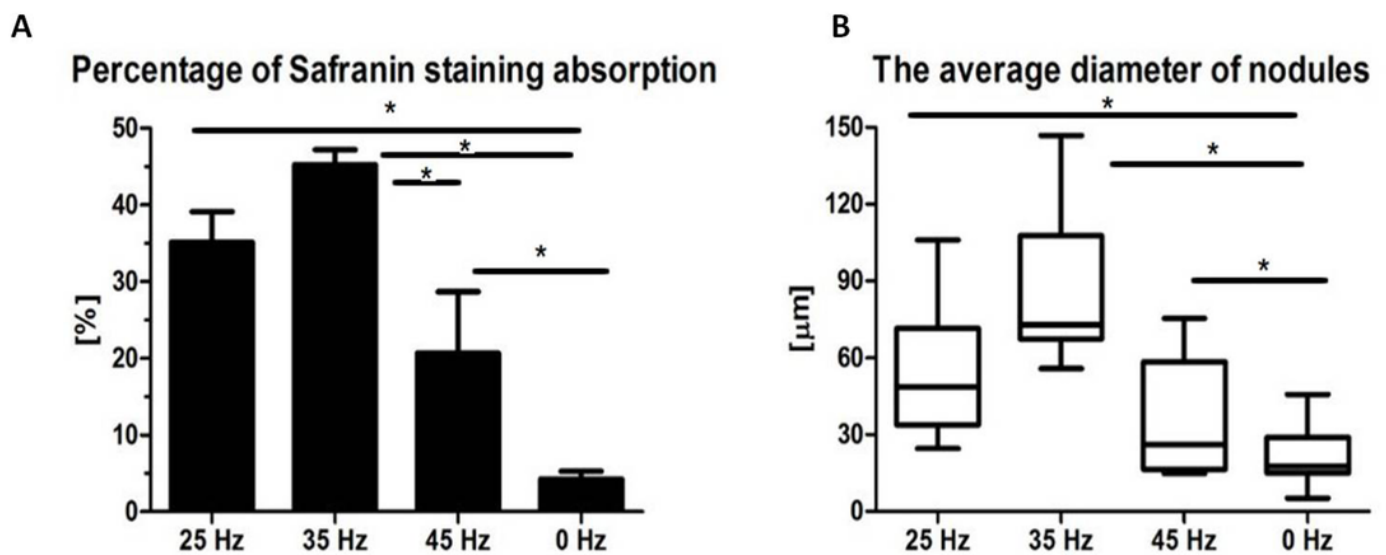
Integrin expression (qPCR)
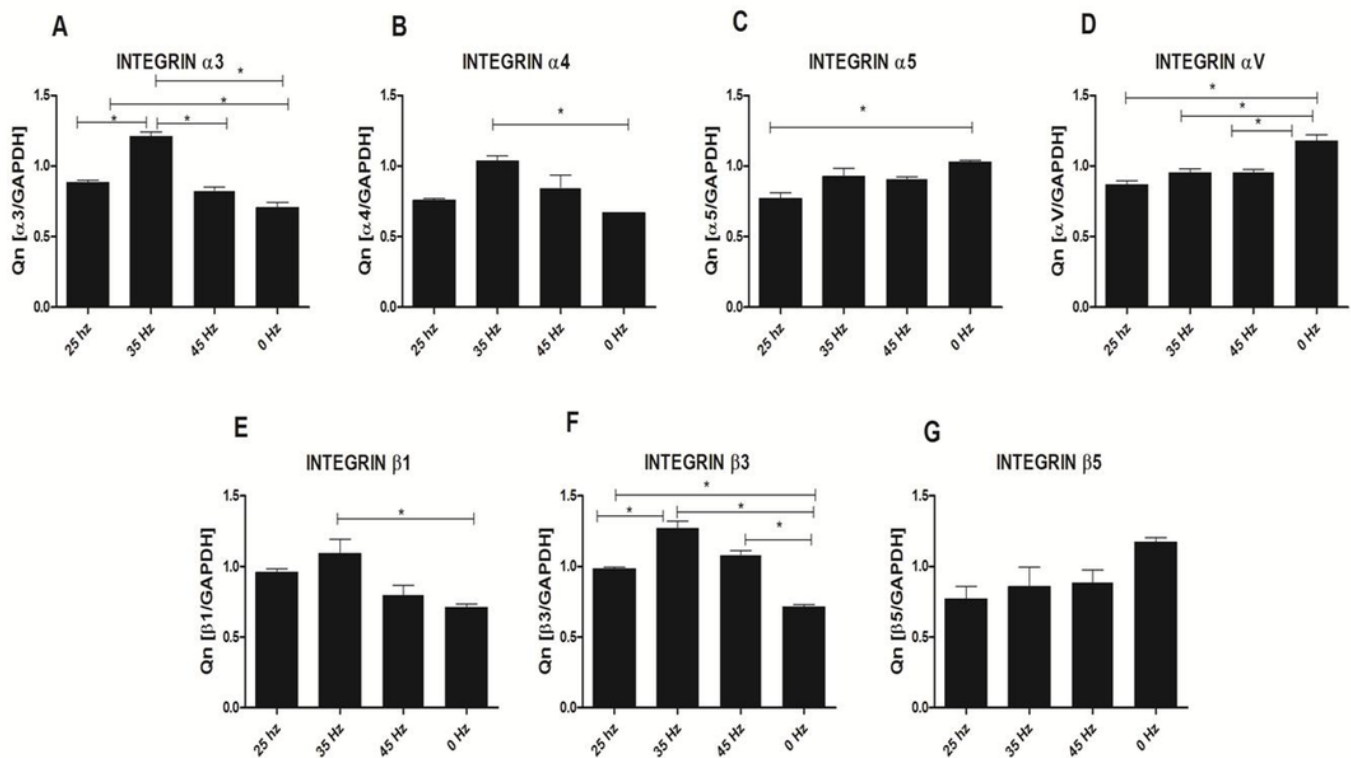
proliferation factor and PDT in adipogenesis
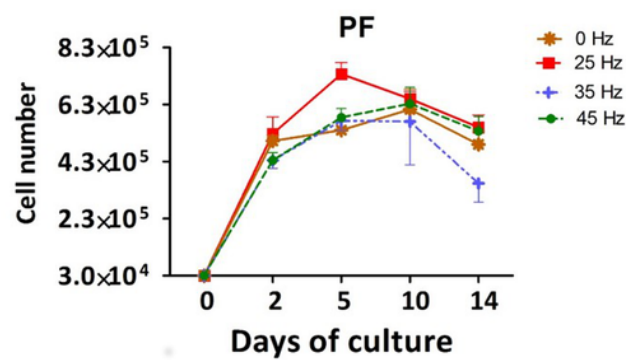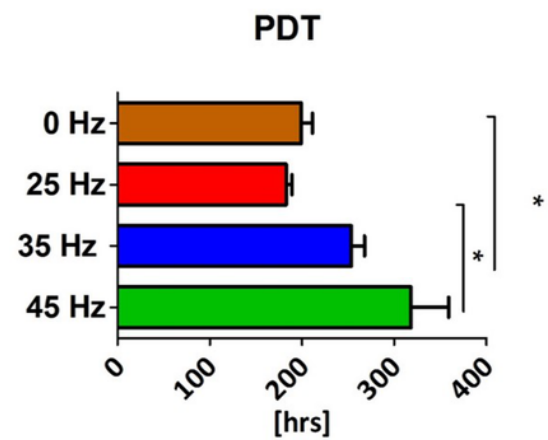
qPCR and morphology oof adipocytes

PANEL A

PANEL B
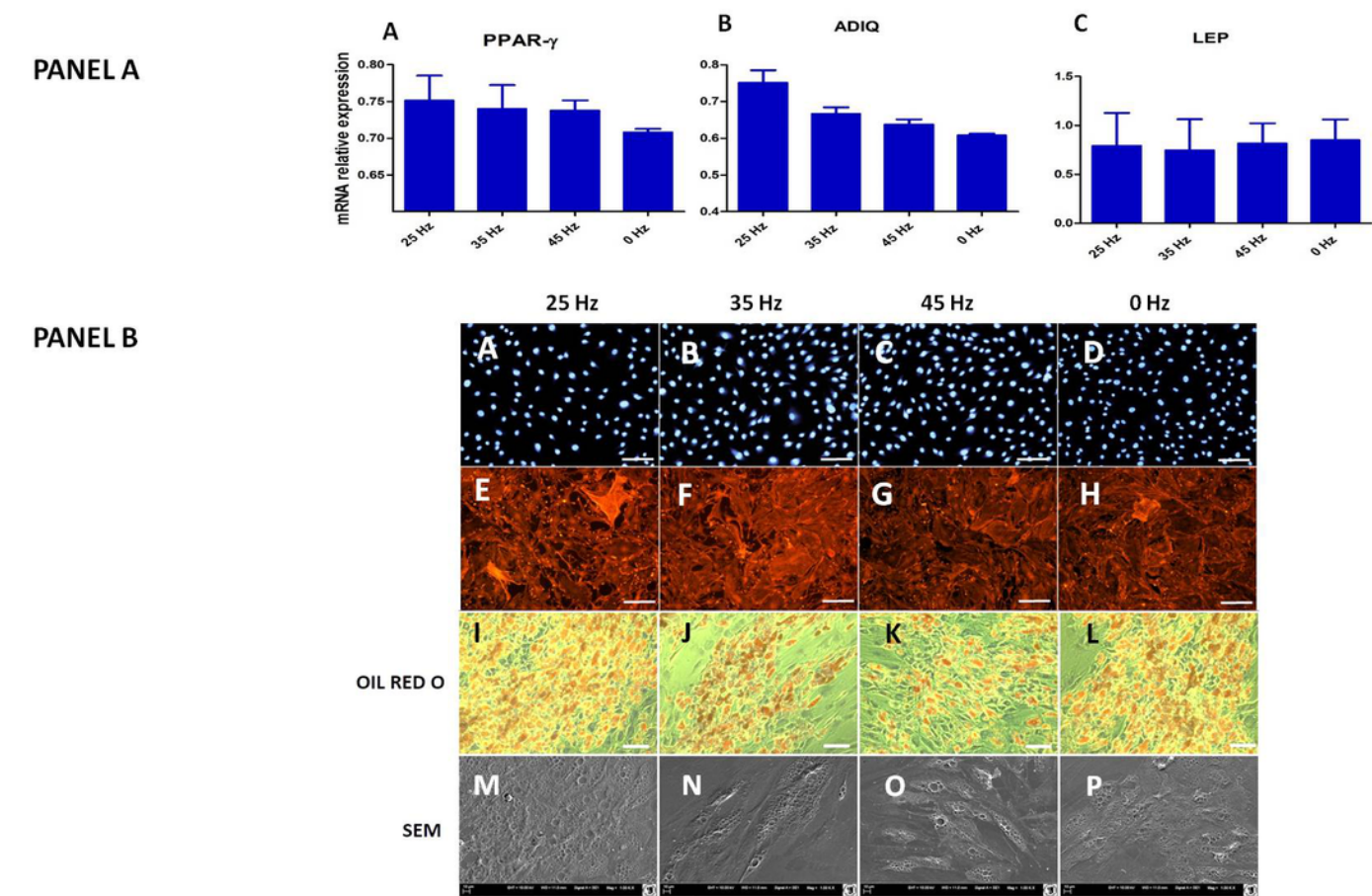
10

Oil red o absorption and adipocytes diameters